

7N-39  
199042  
588

# TECHNICAL NOTE

## D-400

ANALYSIS OF FRAME-REINFORCED CYLINDRICAL SHELLS

PART I - BASIC THEORY

By Richard H. MacNeal and John A. Bailie

Lockheed Aircraft Corporation  
California Division  
Burbank, California

NATIONAL AERONAUTICS AND SPACE ADMINISTRATION

WASHINGTON

May 1960

(NASA-TN-D-400) ANALYSIS OF  
FRAME-REINFORCED CYLINDRICAL SHELLS. PART 1:  
BASIC THEORY (Lockheed Aircraft Corp.)  
58 p

N89-70855

Unclas  
00/39 0199042

1N

NATIONAL AERONAUTICS AND SPACE ADMINISTRATION

TECHNICAL NOTE D-400

ANALYSIS OF FRAME-REINFORCED CYLINDRICAL SHELLS

PART I - BASIC THEORY <sup>1</sup>

By Richard H. MacNeal and John A. Bailie

SUMMARY

L-1028

The state of stress in and near a reinforced frame subjected to concentrated loads and moments and supported in a circular cylindrical shell is investigated and shown to be mainly dependent upon a single parameter. The theoretical approach is new and enables tables of coefficients for the calculation of loads per inch in the shell as well as loads and deflections in the frame to be evaluated using a digital computer. The tables are presented in Part III of this report.

A comparison of this work and two existing theories is made to show relationships between parameters developed in the three methods of analysis. The usefulness of these two theories is thereby extended. Although mainly applicable to airplane fuselages, the results can be applied to problems involving cylindrical shells whose thicknesses are small compared to their diameters, such as ballistic missile bodies.

INTRODUCTION

The analysis of stress distribution in a flexible-frame-supported cylindrical shell, when the shell's frame is subjected to concentrated loads, is a problem of considerable complexity. There are two approaches for the solution: One is to take advantage of the advances in high speed computers to make a complete redundant analysis; the other is to develop a method which is simple and quick to apply, and which promotes deeper understanding of the problem. This latter approach, although lacking precision due to the simplified assumptions involved, is the one adopted in this report.

Wignot, Combs, and Ensrud (ref. 1) developed the first theoretical solution to the problem. Their model of the shell assumes that there are no frames, except the loaded frame, that the longerons are infinitely rigid for axial loads and infinitely flexible for bending loads and the shear panels have uniform shear stiffness. In this solution, the perturbations from the Engineers Bending Theory are assumed to die out within a "length to the undistorted section"  $L$ , which is chosen empirically. Many curves, giving the loads and deflections in the loaded frame as a function of one parameter, are included. Shortly after this work (ref. 1), Hoff presented an analysis (ref. 2) based on the assumption

---

<sup>1</sup>Originally prepared as LMSD 49732, Lockheed Missiles and Space Division, Sunnyvale, California, and reproduced in original form by NASA, by agreement with Lockheed Aircraft Corporation, to increase availability.

that all the unknown quantities are harmonic in the polar angle of the shell and the unknown coefficients are evaluated by a strain energy technique. The structural model of the shell in references 2, 3 and 4 allows for axial and bending stresses in the shell, and considers the shell frames to be equally spaced and to have moments of inertia equal to that of the loaded frame. The ideas presented by Hoff enabled Duberg and Kempner, by the use of recurrence formulas (ref. 3), to present curves giving the loads in the shell as a function of two parameters (ref. 4).

The model adopted in the present report (the first of three reports on shell analysis) is similar to that of references 2, 3, and 4, with the exception that the frames which are not loaded externally are assumed to be "smeared out" in the axial direction, producing a shell with a circumferential bending stiffness per unit length. It is fully realized that practical structures often bear little similarity to the model suggested. Methods are presented in the appendixes which account for some of the differences between the model and practical shells and results are compared with those of references 1 and 4. The problem of discontinuities of circumferential bending stiffness in the axial direction is solved in reference 6. Reference 7 provides a large number of tables from which the loads and deflections can be computed. It also contains suggestions for handling shells which differ from the model in a number of respects.

#### GLOSSARY OF SYMBOLS

A	$2.25/\gamma^4$ parameter of references 3 and 4
$A_n$	arbitrary constants of equation (39)
$a_n$	$(n^2 - 1)(L_r/L_c)^2/3$
B	$\gamma^2/(L_r/L_c)^2$ parameter of references 3 and 4
$C_{qp}$ , etc.	coefficients describing loads in shell and loads and displacements in the loaded frame (see equations (88) to (95))
$D_{ij}$	elements of the matrix defined in equations (A. 10) and (A. 11)
d	parameter of reference 1
E	Young's modulus, lbs/in <sup>2</sup>
$E_{pn}$ , etc.	arbitrary constants in equation (B-1)
e	base of natural (Naperian) logarithms
F	axial force in loaded frame (lbs)
f	transverse load per inch in shell (lbs/in.)

G	shear modulus (lbs/in <sup>2</sup> )
G <sub>1n</sub> , etc.	arbitrary constants in equations (34) and (35)
g	eccentricity between shell and loaded frame's neutral axis (ins.)
I	moment of inertia of a typical unloaded frame (in <sup>4</sup> )
I <sub>ℓ</sub>	moment of inertia of frame at $x = \ell$ (in <sup>4</sup> )
I <sub>o</sub>	moment of inertia of the loaded frame (in <sup>4</sup> )
I	$I/\ell_o$ (in <sup>3</sup> )
j	$\sqrt{-1}$
K <sub>n</sub>	$n \sqrt{n^2 - 1} (1 + 2a_n) / 2 \sqrt{3} \sqrt{1 + a_n}$
L	distance from loaded frame to undistorted shell section (in.)
L <sub>c</sub>	characteristic length (see Glossary) = $r [t' r^2 / i]^{1/4} / \sqrt{6}$ (in.)
L <sub>r</sub>	characteristic length (see Glossary) = $r \sqrt{Et' / Gt} / 2$ (in.)
ℓ <sub>o</sub>	frame spacing (in.)
M	bending moment in the loaded frame (in.-lbs)
M <sub>o</sub>	externally applied concentrated moment (in.-lbs)
m	bending moment per inch in the shell (in.-lbs/in.)
N <sub>c</sub>	constant defined in equation (38)
n	index of harmonic dependance in the $\phi$ direction
P <sub>o</sub>	externally applied concentrated radial load (lbs)
p	axial load per inch in shell (lbs/in.)
P <sub>1</sub> , etc.	roots of the characteristic equation (equations 23 to 26)
q	shear flow in skin (lbs/in.)
Δq	shear flow applied to the frame (lbs/in.)
r	radius of the skin line (in.)
S	transverse shear in the loaded frame (lbs)

s	transverse shear per inch in shell (lbs/in.)
$T_o$	externally applied concentrated tangential load (lbs)
t	skin panel thickness (in.)
$t'$	effective skin panel thickness for axial loads (in.)
u	axial displacement of shell (in.)
v	tangential displacement (in.)
$v_{N.A.}$	tangential displacement at shell neutral axis, when eccentricity between shell and frame neutral axis is considered (in.)
w	radial displacement (in.)
x	axial co-ordinate of shell (in.)
$Z_{ii}$	matrix elements giving the stress-displacement relations at free end of a semi-infinite shell
$\alpha_n$	real part of the complex roots of the characteristic equation
$\beta_n$	imaginary part of the complex roots of the characteristic equation
$\alpha_{1n}, \alpha_{2n}$	real roots of the characteristic equation
$\gamma$	"beef-up" parameter = $I_o/2iL_c$
$\theta$	rotational displacement of the loaded frame
$\Theta$	$Ei(n^3 - n)^2 / Gtr^4$
$\Lambda$	$n^2(n^3 - n)^2 i / t' r^6$
$\phi$	polar co-ordinate of frames and shell
$\eta$	$g/r$ - eccentricity parameter
-	denotes symmetric harmonic coefficient
=	denotes antisymmetric harmonic coefficient

When an expression holds for both cases, the symmetric case is derived.

## GLOSSARY OF TERMINOLOGY

The terms "Input Impedance" and "Characteristic Length" are frequently used in this report. They are defined as follows:

Input Impedance is the relationship between the tangential displacement and shear flow harmonic coefficients of the shell at the section of the loaded frame.

Characteristic Length. In this report there are two characteristic lengths defined as follows: (1)  $L_c$  is the distance required for the exponential envelope of the lowest-order, self-equilibrating stress system to decay to  $1/e$  of its value at  $x = 0$ , provided that the skin panels are rigid in shear. (2)  $L_b$  is the distance required for the envelope of the lowest-order, self-equilibrating stress system to decay to  $1/e$  of its value at  $x = 0$ , provided that the frames are rigid in bending.

## A REINFORCED LOADED FRAME IN AN INFINITE, UNIFORM SHELL

## Plan of the Report

In this part of the report, analytical solutions are obtained describing the state of stress in and near a reinforced frame subjected to concentrated loads and situated in an infinite, uniform, circularly-cylindrical shell. These solutions, and the mathematical analysis leading to them, form a basis for developments in the rest of the report and in references 6 and 7.

Many reinforced shells contain longitudinal members, called longerons, carrying most of the direct stress. If the total direct-stress-carrying area of both skin and longerons is divided by the circumference, an effective skin thickness resisting direct stresses is derived. The process of finding the contribution of the longerons to the effective thickness is described as "smearing out" the longerons.

In these analyses, the longerons are assumed to be "smeared out", producing a uniform shell with thickness,  $t$ , for shear loads and thickness,  $t'$ , for axial loads. In addition, the frames that are not externally loaded are "smeared out" in the axial direction to produce a circumferential bending stiffness,  $Ei$ , per unit length. The bending stiffness of the externally-loaded frame is not "smeared out". The advantages claimed for this approach are:

- (1) A simplification of the mathematical process involved in getting a solution. Previous solutions were only partly analytic in that certain coefficients could be obtained only in numerical form. The simplification of the results promotes clearer insight into the processes involved. It also permits easier extension to more difficult problems.

- (2) Elimination of one parameter in plotting solutions. In references 3 and 4, two parameters were required in order to describe the properties of a uniform shell. In the present analysis, two parameters are required to describe the properties of a shell in which the loaded frame may be reinforced. For shells typified by conventional transport airplane construction and ballistic missile bodies, only one of these parameters is important.

In "smearing out" the shell frames, but not the loaded frame, the effect of finite frame spacing on the solutions is eliminated. This effect is treated in Appendix A, where it is shown that a simple approximate correction gives good results for most practical cases.

The loads and deflections in the shell and loaded frame are shown in figures 1 and 2.

#### Assumptions

- (1) The loaded frame has in-plane bending flexibility. It is perfectly free to warp out of its plane and to twist. It has no extensional or shearing flexibilities.
- (2) The effect of the eccentricity of the skin attachment with respect to the frame neutral axis is ignored.
- (3) The shell consists of skin, longerons, and frames similar to the loaded frame (but possibly with different moments of inertia). The skin and longerons have no bending stiffness.
- (4) The longerons are "smeared out" over the circumference giving an equivalent thickness,  $t'$ , (including effective skin) for axial loads.
- (5) The shell frames are "smeared out" in the axial direction, giving an equivalent moment of inertia per inch,  $i$ , for circumferential bending loads.

#### Method of Solution

An exploded view of the shell is shown in figure 3.

- (1) Partial differential equations are written describing relationships between internal forces and displacements in the shell.
- (2) Dependence of all unknown quantities on the polar angle  $\phi$  (see fig. 1) is assumed to be harmonic. For example

$$q = \sum_{n=1}^{\infty} \bar{q}_n \sin n\phi - \sum_{n=0}^{\infty} \bar{\bar{q}}_n \cos n\phi$$

This step reduces the partial differential equations of step (1) to ordinary differential equations in  $x$  (with  $n$  as a parameter) which are combined and solved.

- (3) Since the shell is symmetrical with respect to the plane  $x = 0$ , the axial displacement,  $u$ , is planar for  $x = 0$ . This boundary condition permits a definite expression to be written between the shear flow harmonic coefficients,  $\bar{q}_n$ , and the tangential displacement harmonic coefficients,  $\bar{v}_n$ , at  $x = 0$ .
- (4) Another relationship involving  $\bar{q}_n$ ,  $\bar{v}_n$ , and the applied concentrated loads is obtained for the loaded frame, analyzed as a free ring.
- (5) Combination of the expressions obtained in steps (3) and (4) results in the determination of  $\bar{q}_n$  and all other harmonic coefficients in terms of applied loads.
- (6) The complete solution is synthesized from the harmonic coefficients. The "elementary beam theory" part of the solution ( $n = 0, 1$ ) is treated separately from the self-equilibrating part ( $n = 2, 3, 4, \dots$ ).

### Partial Differential Equations of the Shell

Equations are written with reference to the infinitesimal element of shell, shown in figure 4.

#### Equations of Equilibrium

$$\frac{\partial p}{\partial x} - \frac{1}{r} \frac{\partial q}{\partial \phi} = 0 \quad (1)$$

$$\frac{1}{r} \frac{\partial f}{\partial \phi} - \frac{\partial q}{\partial x} - \frac{s}{r} = 0 \quad (2)$$

$$\frac{\partial s}{\partial \phi} + f = 0 \quad (3)$$

$$\frac{\partial m}{\partial \phi} - s r = 0 \quad (4)$$



### Stress-Strain Relationships

$$p = Et' \frac{\partial u}{\partial x} \quad (5)$$

$$q = -Gt \left( \frac{1}{r} \frac{\partial u}{\partial \phi} + \frac{\partial v}{\partial x} \right) \quad (6)$$

$$\frac{\partial \theta}{\partial \phi} = -\frac{mr}{Ei} \quad (7)$$

### Strain-Displacement Relationships

$$\frac{\partial w}{\partial \phi} = \theta r - v \quad (8)$$

$$\frac{\partial v}{\partial \phi} = w \quad (9)$$

### Derived Relationship Between Shear Flow and Tangential Displacement

Combine equations (7), (8) and (9):

$$\frac{mr}{Ei} = -\frac{1}{r} \left( \frac{\partial v}{\partial \phi} + \frac{\partial^3 v}{\partial \phi^3} \right) \quad (10)$$

Combine equations (2), (3) and (4):

$$\frac{\partial q}{\partial x} = -\frac{1}{r^2} \left( \frac{\partial^3 m}{\partial \phi^3} + \frac{\partial m}{\partial \phi} \right) \quad (11)$$

Combine equations (10) and (11):

$$\frac{\partial q}{\partial x} = \frac{Ei}{r^4} \left( \frac{\partial^3}{\partial \phi^3} + \frac{\partial}{\partial \phi} \right)^2 v \quad (12)$$

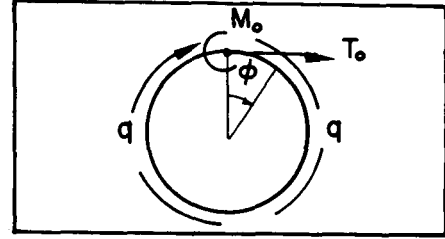
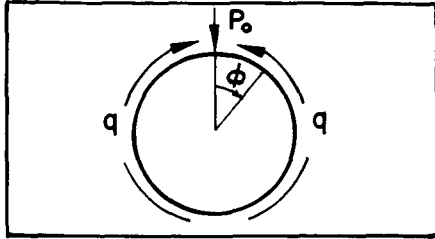
Equations (1), (5), (6), and (12) are written in terms of the variables  $p$ ,  $q$ ,  $u$ , and  $v$ , which are of primary importance in all parts of the report.

### Introduction of Harmonic Coefficients

The solution to any problem concerned with the shell is periodic with period  $2\pi$  in the polar angle  $\phi$ . Hence, all unknown quantities may be expanded by Fourier series in  $\phi$ .

It is convenient to consider the symmetry of the solutions with respect to  $\phi = 0$ . For a unit radial load at  $\phi = 0$  (see fig. 1) solutions will be symmetrical with respect

to  $\phi = 0$ , while for unit tangential or moment loads they will be antisymmetrical as shown below:



$$\left. \begin{aligned} p &= \sum_{n=0}^{\infty} \bar{p}_n \cos n\phi; \quad q = \sum_{n=1}^{\infty} \bar{q}_n \sin n\phi \\ u &= \sum_{n=0}^{\infty} \bar{u}_n \cos n\phi; \quad v = \sum_{n=1}^{\infty} \bar{v}_n \sin n\phi \end{aligned} \right\} \quad (13)$$

$$\left. \begin{aligned} p &= \sum_{n=1}^{\infty} \bar{\bar{p}}_n \sin n\phi; \quad q = -\sum_{n=0}^{\infty} \bar{\bar{q}}_n \cos n\phi \\ u &= \sum_{n=1}^{\infty} \bar{\bar{u}}_n \sin n\phi; \quad v = -\sum_{n=0}^{\infty} \bar{\bar{v}}_n \cos n\phi \end{aligned} \right\} \quad (14)$$

For any particular value of  $n$ , the antisymmetric terms are symmetric with respect to a plane with polar angle  $\phi = \pi/2n$ , since if  $\phi = \phi' + \pi/2n$ , then

$$\begin{aligned} \sin(n\phi) &= \cos(n\phi') \\ -\cos(n\phi) &= \sin(n\phi') \end{aligned}$$

Hence, a homogeneous relationship (one not involving the loads directly) between antisymmetric harmonic coefficients with the same index,  $n$ , will have identical form with the corresponding relationship between symmetric harmonic coefficients.

Substitute equation (13) into equations (12), (1), (15) and (6) and obtain relationships between symmetric harmonic coefficients of a particular order. Repeat, using equation (14) instead of (13), to obtain the antisymmetric harmonic coefficients. In so doing, make use of the following identities:

$$\left. \begin{aligned} \left( \frac{\partial^3}{\partial \phi^3} + \frac{\partial}{\partial \phi} \right)^2 \sin n\phi &= -(n^3 - n)^2 \sin n\phi \\ \left( \frac{\partial^3}{\partial \phi^3} + \frac{\partial}{\partial \phi} \right)^2 \cos n\phi &= -(n^3 - n)^2 \cos n\phi \end{aligned} \right\} \quad (15)$$

The results are:

$$\left. \begin{aligned} \frac{d\bar{q}_n}{dx} &= -\frac{Ei}{r^4} (n^3 - n)^2 \bar{v}_n \\ \frac{d\bar{\bar{q}}_n}{dx} &= -\frac{Ei}{r^4} (n^3 - n)^2 \bar{\bar{v}}_n \end{aligned} \right\} \quad (16)$$

$$\left. \begin{aligned} \frac{d\bar{p}_n}{dx} - \frac{n}{r} \bar{q}_n &= 0 \\ \frac{d\bar{\bar{p}}_n}{dx} - \frac{n}{r} \bar{\bar{q}}_n &= 0 \end{aligned} \right\} \quad (17)$$

$$\left. \begin{aligned} \bar{p}_n &= Et' \frac{d\bar{u}_n}{dx} \\ \bar{\bar{p}}_n &= Et' \frac{d\bar{\bar{u}}_n}{dx} \end{aligned} \right\} \quad (18)$$

$$\left. \begin{aligned} \bar{q}_n &= Gt \left( \frac{n}{r} \bar{u}_n - \frac{d\bar{v}_n}{dx} \right) \\ \bar{\bar{q}}_n &= Gt \left( \frac{n}{r} \bar{\bar{u}}_n - \frac{d\bar{\bar{v}}_n}{dx} \right) \end{aligned} \right\} \quad (19)$$

It is evident that it is sufficient to consider symmetrical coefficients alone, except for relationships involving applied loads; the results will also apply for antisymmetrical coefficients. In the work that follows, where both types of coefficients exist only the symmetrical one is indicated. It is now known that the equations for the antisymmetrical case have the identical form, but they are omitted for conciseness.

#### Formulation and Solution of the Characteristic Equation of the Shell

Equations (16) through (19) are first combined to obtain a single equation.

Differentiate equation (19) and substitute from equations (16) and (18) to yield

$$\frac{d\bar{q}_n}{dx} = Gt \left[ \frac{n}{r} \cdot \frac{\bar{p}_n}{Et'} + \frac{r^4}{Ei (n^3 - n)^2} \frac{d^3 \bar{q}_n}{dx^3} \right] \quad (20)$$

Differentiate (20), substitute from equation (17), and rearrange to give:

$$\frac{d^4 \bar{q}_n}{dx^4} - \frac{Ei(n^3 - n)^2}{Gtr^4} \cdot \frac{d^2 \bar{q}_n}{dx^2} + \frac{n^2(n^3 - n)^2 i}{t'r^6} q_n = 0 \quad (21)$$

The general solutions of this equation are exponential functions of the roots of the characteristic equation which is:

$$p^4 - \theta p^2 + \lambda = 0 \quad (22)$$

where

$$\theta = \frac{Ei(n^3 - n)^2}{Gtr^4}$$

$$\lambda = \frac{n^2(n^3 - n)^2 i}{t'r^6}$$

Equation (22) is a biquadratic equation, so that there is no difficulty in obtaining the roots.

$$\begin{aligned} p^2 &= \theta/2 \pm j \sqrt{\lambda - (\theta/2)^2} \quad \text{for } \lambda > (\theta/2)^2 \\ &= \theta/2 \pm \sqrt{(\theta/2)^2 - \lambda} \quad \text{for } \lambda < (\theta/2)^2 \end{aligned}$$

Using identities 58.1 and 58.2 of reference 5, we have:

For  $\lambda > (\theta/2)^2$

$$p_1 = -p_3 = -\sqrt{\frac{\sqrt{\lambda} + \theta/2}{2}} - j \sqrt{\frac{\sqrt{\lambda} - \theta/2}{2}} = -\alpha - j\beta \quad (23)$$

$$p_2 = -p_4 = -\sqrt{\frac{\sqrt{\lambda} + \theta/2}{2}} + j \sqrt{\frac{\sqrt{\lambda} - \theta/2}{2}} = -\alpha + j\beta \quad (24)$$

For  $\lambda < (\theta/2)^2$

$$p_1 = -p_3 = -\left[ \frac{\theta}{2} + \sqrt{\left(\frac{\theta}{2}\right)^2 - \lambda} \right]^{\frac{1}{2}} = -\alpha_1 \quad (25)$$

$$p_2 = -p_4 = -\left[ \frac{\theta}{2} - \sqrt{\left(\frac{\theta}{2}\right)^2 - \lambda} \right]^{\frac{1}{2}} = -\alpha_2 \quad (26)$$

For the particular problem at hand in which the shell extends to infinity, solutions corresponding to the roots with positive real part ( $P_3$  and  $P_4$ ) must be discarded for  $x > 0$  and vice versa for  $x < 0$ .

It is important to relate the roots obtained above to the physical properties of the shell in a manner that is both convenient for computation and suggestive of important relationships. The usefulness of the following definitions will be seen later. Define:

$$L_c = \frac{r}{\sqrt{6}} \left[ \frac{t' r^2}{i} \right]^{\frac{1}{4}} \sim \begin{array}{l} \text{the characteristic length} \\ \text{with rigid shear panels} \end{array} \quad (27)$$

$$L_r = \frac{r}{2} \sqrt{\frac{Et'}{Gt}} \sim \begin{array}{l} \text{the characteristic length} \\ \text{with rigid frames} \end{array} \quad (28)$$

Evaluate  $\alpha$  and  $\beta$  from equations (23) and (24) in terms of these coefficients. Since  $\alpha$  and  $\beta$  depend on the harmonic index,  $n$ , a subscript  $n$  is added.

$$\alpha_n = \frac{\lambda^{\frac{1}{4}}}{\sqrt{2}} \left[ 1 + \frac{\theta}{2\sqrt{\lambda}} \right]^{\frac{1}{2}} \quad \beta_n = \frac{\lambda^{\frac{1}{4}}}{\sqrt{2}} \left[ 1 - \frac{\theta}{2\sqrt{\lambda}} \right]^{\frac{1}{2}}$$

now

$$\lambda^{\frac{1}{4}} = \left[ \frac{n^2(n^3 - n)^2 i}{t' r^6} \right]^{\frac{1}{4}} = \frac{n \sqrt{n^2 - 1}}{\sqrt{6} L_c}$$

$$\frac{\theta}{2\sqrt{\lambda}} = \frac{Ei(n^3 - n)^2}{2Gtr^4} \cdot \frac{6L_c^2}{n^2(n^2 - 1)} = \frac{n^2 - 1}{3} \left( \frac{L_r}{L_c} \right)^2$$

Hence

$$\alpha_n = \frac{1}{L_c} \cdot \frac{n \sqrt{n^2 - 1}}{2\sqrt{3}} \cdot \sqrt{1 + \frac{n^2 - 1}{3} \left( \frac{L_r}{L_c} \right)^2} \quad (29)$$

$$\beta_n = \frac{1}{L_c} \cdot \frac{n \sqrt{n^2 - 1}}{2\sqrt{3}} \cdot \sqrt{1 - \frac{n^2 - 1}{3} \left( \frac{L_r}{L_c} \right)^2} \quad (30)$$

In the case of real roots:

$$\left. \begin{matrix} \alpha_{1n} \\ \alpha_{2n} \end{matrix} \right\} = \bigwedge^{\frac{1}{4}} \left[ \frac{\theta}{2\sqrt{\lambda}} \pm \sqrt{\left( \frac{\theta}{2\sqrt{\lambda}} \right)^2 - 1} \right]^{\frac{1}{2}}$$

Define:

$$a_n = \frac{\theta}{2\sqrt{\lambda}} = \frac{n^2 - 1}{3} \left( \frac{L_r}{L_c} \right)^2 \quad (31)$$

then

$$\left. \begin{matrix} \alpha_{1n} \\ \alpha_{2n} \end{matrix} \right\} = \frac{1}{L_c} \cdot \frac{n\sqrt{n^2 - 1}}{\sqrt{6}} \cdot \left[ a_n \pm \sqrt{a_n^2 - 1} \right]^{\frac{1}{2}} \quad (32)$$

It can be shown by direct algebraic manipulation that:

$$\alpha_{1n} + \alpha_{2n} = 2\alpha_n \quad (33)$$

This relationship will be useful later.

The form of the solution for complex roots corresponding to  $x > 0$  is:

$$\bar{q}_n = G_{1n} e^{-\alpha_n x} \cos(\beta_n x + G_{2n}) \quad (34)$$

The form of the solution for real roots corresponding to  $x > 0$  is:

$$\bar{q}_n = G_{3n} e^{-\alpha_{1n} x} + G_{4n} e^{-\alpha_{2n} x} \quad (35)$$

Justification of the term "characteristic length" is obtained from equation (34). If  $L_r$  is set equal to zero and  $n$  is chosen equal to 2, then  $\alpha_n = 1/L_c$  from equation (29). Hence,  $L_c$  is the distance required for the exponential envelope of the lowest order self-equilibrating stress system to decay to  $1/e$  of its value at  $x = 0$ , provided  $L_r = 0$ . For transport fuselage shells,  $L_r/L_c$  is of the order of 0.3. For such a value, it will be observed that, for  $n = 2$ ,  $\alpha_n$  is very nearly equal to  $1/L_c$ .

The justification of the definition of  $L_r$  is obtained by allowing  $i$  to become infinite in equation (20). The roots of the characteristic equation then become

$$P_r = \pm n/2 L_r \quad (36)$$

The solution, valid for  $x > 0$  and corresponding to these roots, is:

$$(\bar{q}_n)_r = G_{rn} e^{-nx/2 L_r} \quad (37)$$

Hence,  $L_r$  is the distance required for the envelope of the lowest-order, self-equilibrating stress system to decay to  $1/e$  of its value at  $x = 0$ , provided that the frames are rigid.

For  $L_r$  and  $L_c$  not equal to zero, the form of the solution will change from decaying sinusoid to exponential type for  $n$  sufficiently large. The critical value of harmonic index for which this transition occurs is, from equation (30):

$$N_c = \sqrt{1 + 3 \left( \frac{L_c}{L_r} \right)^2} \quad (38)$$

It will also be observed in equation (29) that for  $n = 0$  and for  $n = 1$ ,  $\alpha_n$  and  $\beta_n$  are zero. This means that the corresponding terms in the solution experience no decay for increasing  $x$ . These terms are, in fact, just those that would be predicted by elementary beam theory. Their effect will be added to the solution at the very end.

**Introduction of Boundary Conditions. The Relationship Between Tangential Shear Flow and Tangential Displacement Harmonic Coefficients at  $x = 0$**

At  $x = 0$ , axial displacement is planar due to the symmetry of the shell. Hence,  $\bar{u}_n = 0$  for  $n \geq 2$ .  $\bar{p}_n$ ,  $\bar{u}_n$ , and  $\bar{v}_n$  satisfy equation (21) as well as  $\bar{q}_n$ , so that the forms of solution given in equations (34) and (35) are valid for all quantities.

Hence:

$$\bar{u}_n = A_n e^{-\alpha_n x} \sin \beta_n x \quad n < N_c \quad (39a)$$

$$\bar{u}_n = A_n \left( e^{-\alpha_1 n x} - e^{-\alpha_2 n x} \right) \quad n > N_c \quad (39b)$$

$\bar{p}_n$  can be obtained using equation (18), and  $\bar{q}_n$  can then be obtained using equation (17):

$$\bar{p}_n = Et' A_n e^{-\alpha_n x} \left[ -\alpha_n \sin \beta_n x + \beta_n \cos \beta_n x \right] \quad \text{for } n < N_c \quad (40a)$$

$$\bar{p}_n = Et' A_n \left[ -\alpha_{1n} e^{-\alpha_{1n} x} + \alpha_{2n} e^{-\alpha_{2n} x} \right] \quad \text{for } n > N_c \quad (40b)$$

(continued)

$$\bar{q}_n = A_n Et' \frac{r}{n} e^{-\alpha_n x} \left[ (\alpha_n^2 - \beta_n^2) \sin \beta_n x - 2\alpha_n \beta_n \cos \beta_n x \right] \text{ for } n < N_c \quad (41a)$$

$$\bar{q}_n = A_n Et' \frac{r}{n} \left[ \alpha_{1n}^2 e^{-\alpha_{1n} x} - \alpha_{2n}^2 e^{-\alpha_{2n} x} \right] \text{ for } n > N_c \quad (41b)$$

Evaluate  $A_n$  in terms of  $q_n(0)$ , the shear flow coefficient at  $x = 0$ :

$$A_n = -\frac{n}{r} \cdot \frac{1}{Et'} \cdot \frac{\bar{q}_n(0)}{2\alpha_n \beta_n} \text{ for } n < N_c \quad (42a)$$

$$A_n = \frac{n}{r} \cdot \frac{1}{Et'} \cdot \frac{q_n(0)}{(\alpha_{1n}^2 - \alpha_{2n}^2)} \text{ for } n > N_c \quad (42b)$$

Substituting equations (42a) and (42b) into (41a) and (41b), respectively, gives

$$\bar{q}_n = \bar{q}_n(0) e^{-\alpha_n x} \left[ \cos \beta_n x - \frac{(\alpha_n^2 - \beta_n^2)}{2\alpha_n \beta_n} \sin \beta_n x \right] \text{ for } n < N_c \quad (43a)$$

$$\bar{q}_n = \bar{q}_n(0) \left[ \frac{\alpha_{1n}^2 e^{-\alpha_{1n} x}}{(\alpha_{1n}^2 - \alpha_{2n}^2)} - \frac{\alpha_{2n}^2 e^{-\alpha_{2n} x}}{(\alpha_{1n}^2 - \alpha_{2n}^2)} \right] \text{ for } n > N_c \quad (43b)$$

Evaluate  $\bar{v}_n$  from equation (16):

$$\bar{v}_n = \frac{r^4 \bar{q}_n(0)}{Ei(n^3 - n)^2} e^{-\alpha_n x} \left[ \left\{ \alpha_n + \frac{(\alpha_n^2 - \beta_n^2)}{2\alpha_n} \right\} \cos \beta_n x + \left\{ \beta_n - \frac{(\alpha_n^2 - \beta_n^2)}{2\beta_n} \right\} \sin \beta_n x \right] \text{ for } n < N_c \quad (44a)$$

$$\bar{v}_n = \frac{r^4 \bar{q}_n(0)}{Ei(n^3 - n)^2} \left[ \frac{\alpha_{1n}^3 e^{-\alpha_{1n} x}}{(\alpha_{1n}^2 - \alpha_{2n}^2)} - \frac{\alpha_{2n}^3 e^{-\alpha_{2n} x}}{(\alpha_{1n}^2 - \alpha_{2n}^2)} \right] \text{ for } n > N_c \quad (44b)$$



The relationship between  $\bar{v}_n(o)$  and  $\bar{q}_n(o)$  will be used in conjunction with a similar relationship for the loaded frame to solve the combined problem.

$$\frac{\bar{v}_n(o)}{\bar{q}_n(o)} = \frac{r^4}{Ei(n^3 - n)^2} \cdot \frac{3\alpha_n^2 - \beta_n^2}{2\alpha_n} \quad \text{for } n < N_c \quad (45a)$$

$$= \frac{r^4}{Ei(n^3 - n)^2} \cdot \left( \frac{\alpha_{1n}^3 - \alpha_{2n}^3}{\alpha_{1n}^2 - \alpha_{2n}^2} \right) \quad \text{for } n > N_c \quad (45b)$$

It can be shown that equations (45a) and (45b) are formally identical. Define:

$$K_n = L_c \left( \frac{3\alpha_n^2 - \beta_n^2}{2\alpha_n} \right) = \frac{n\sqrt{n^2 - 1}}{2\sqrt{3}} \cdot \frac{1 + 2a_n}{\sqrt{1 + a_n}} \quad (46)$$

See glossary of symbols for definition of  $a_n$ . Also define:

$$K_n^* = L_c \left( \frac{\alpha_{1n}^3 - \alpha_{2n}^3}{\alpha_{1n}^2 - \alpha_{2n}^2} \right) = L_c \left( \frac{\alpha_{1n}^2 + \alpha_{1n}\alpha_{2n} + \alpha_{2n}^2}{\alpha_{1n} + \alpha_{2n}} \right) \quad (47)$$

Using equation (33) in (47) and simplifying,

$$K_n^* = \frac{n\sqrt{n^2 - 1}}{2\sqrt{3}} \cdot \frac{1 + 2a_n}{\sqrt{1 + a_n}} = K_n \quad (48)$$

The form of the relationship between tangential displacement and tangential shear flow, the input impedance, is, therefore, the same for all  $n \geq 2$ , and is:

$$\frac{\bar{v}_n(o)}{\bar{q}_n(o)} = \frac{r^4}{Ei(n^3 - n)^2} \cdot \frac{K_n}{L_c} \quad (49)$$

Note that  $K_n = 1$  for  $n = 2$  and  $L_r/L_c = 0$ .

Since the form of the relationship between the symmetric and antisymmetric harmonic coefficients is identical, equation (49) is also valid for antisymmetric cases.

Equations for the Loaded Frame

The differential equations for the loaded frame are similar in form to the relevant equations for the shell. The net shear flow,  $\Delta q$ , is equal to  $q(o^+) - q(o^-)$ , and acts on the frame.

Equations of Equilibrium

$$\frac{1}{r} \frac{dF}{d\phi} - \Delta q - \frac{S}{r} + \frac{t_a}{r} = 0 \tag{50}$$

$$\frac{dS}{d\phi} + F + p_a = 0 \tag{51}$$

$$\frac{dM}{d\phi} - S r - m_a = 0 \tag{52}$$

Stress-Strain Relationship

$$\frac{d\theta}{d\phi} = - \frac{Mr}{EI_o} \tag{53}$$

Strain-Displacement Relationships

$$\frac{dw}{d\phi} = - v + \theta r \tag{54}$$

$$\frac{dv}{d\phi} = w \tag{55}$$

The above equations are combined in order to give the net shear flow in terms of tangential displacement and applied loads.

Combine equations (53), (54) and (55):

$$\frac{Mr}{EI_o} = - \frac{d\theta}{d\phi} = - \frac{1}{r} \left( \frac{dv}{d\phi} + \frac{d^3 v}{d\phi^3} \right) \tag{56}$$

Combine equations (50), (51) and (52):

$$\Delta q = - \frac{1}{r^2} \left( \frac{d^3 M}{d\phi^3} + \frac{dM}{d\phi} \right) + \frac{1}{r^2} \left( \frac{d^2 m_a}{d\phi^2} + m_a \right) - \frac{1}{r} \frac{dp_a}{d\phi} + \frac{t_a}{r} \tag{57}$$

L-1028

Combine equations (56) and (57):

$$\Delta q = \frac{EI_o}{r^4} \left( \frac{d^3}{d\phi^3} + \frac{d}{d\phi} \right)^3 v + \frac{1}{r} \left( \frac{d^2 m_a}{d\phi^2} + m_a \right) - \frac{1}{r} \frac{dp_a}{d\phi} + \frac{t_a}{r} \quad (58)$$

#### Calculation of Shear Flow Harmonic Coefficients

For the case of concentrated loads applied at  $\phi = 0$  (see fig. 1), the distributed loads  $p_a$ ,  $t_a$ , and  $m_a$  can be represented by the following Fourier expansions in  $\phi$ :

Symmetric Case  $m_a = t_a = 0$

$$\begin{aligned} p_a &= \sum_{n=0}^{\infty} \bar{p}_{an} \cos n\phi \\ &= \frac{P_o}{2\pi} + \frac{P_o}{\pi} \sum_{n=1}^{\infty} \cos n\phi \end{aligned} \quad (59)$$

Antisymmetric Case  $p_a = 0$

$$m_a = \sum_{n=0}^{\infty} \bar{m}_{an} \cos n\phi = \frac{M_o}{2\pi} + \frac{M_o}{\pi} \sum_{n=1}^{\infty} \cos n\phi \quad (60)$$

$$t_a = \sum_{n=0}^{\infty} \bar{t}_{an} \cos n\phi = \frac{T_o}{2\pi} + \frac{T_o}{\pi} \sum_{n=1}^{\infty} \cos n\phi \quad (61)$$

The above Fourier expansions do not converge. However, results based on them do converge to the correct values.

Introduce harmonic coefficients from equations (13) and (14) into equation (58) using equation (15).

Symmetric Case

$$\bar{\Delta q}_n = -\frac{EI_o}{r^4} (n^3 - n)^2 \bar{v}_n + \frac{nP_o}{\pi r} \quad \text{for } n \geq 1 \quad (62)$$

(continued)

For  $n \geq 2$ ,  $\overline{\Delta q_n} = 2 \overline{q_n}(o)$

Hence, 
$$\overline{q_n}(o) = - \frac{EI_o}{2r^4} (n^3 - n)^2 \overline{v}_n + \frac{nP_o}{\pi r} \quad \text{for } n \geq 2 \quad (62a)$$

Antisymmetric Case

$$\overline{\overline{q_n}}(o) = - \frac{EI_o}{2r^4} (n^3 - n)^2 \overline{\overline{v}}_n - \frac{(1 - n^2)M_o}{2\pi r^2} - \frac{T_o}{2\pi r} \quad (63)$$

Equations (62) and (63) can be combined with equation (49) to give the shear flow coefficients in terms of applied load:

Symmetric Case

$$\overline{q_n}(o) = - \frac{EI_o}{2Ei} \cdot \frac{K_n}{L_c} \overline{q_n}(o) + \frac{nP_o}{2\pi r} \quad \text{for } n \geq 2 \quad (64)$$

Define:

$$\gamma = \frac{I_o}{2iL_c} \quad (65)$$

$\gamma$  is a measure of the bending stiffness of the loaded frame relative to the bending stiffness of the shell.

Then

$$\overline{q_n}(o) = \frac{\frac{nP_o}{2\pi r}}{1 + \gamma K_n} \quad (66)$$

Antisymmetric Case

$$\overline{\overline{q_n}}(o) = - \frac{\frac{1}{2\pi} \left\{ \frac{T_o}{r} + \frac{(1 - n^2)}{r^2} M_o \right\}}{1 + \gamma K_n} \quad (67)$$

$K_n$ , which increases as  $n^3$  for large  $n$ , provides fairly rapid decrement of these expressions. Equations (43a) and (43b) can be used to obtain the shear flow coefficients for  $x > 0$ .

Equations (66) and (67) are used to generate the entire solution to the problem.

### Axial Load Harmonic Coefficients

The harmonic coefficients for axial load per inch can be obtained from  $q_n(o)$  as follows, substituting equation (42) into equation (40):

$$\bar{p}_n = -\bar{q}_n(o) \frac{ne^{-\alpha_n x}}{2r\alpha_n} \left( \cos \beta_n x - \frac{\alpha_n}{\beta_n} \sin \beta_n x \right) \quad \text{for } n < N_c \quad (68)$$

$$\bar{p}_n = -\bar{q}_n(o) \frac{n}{r(\alpha_{1n}^2 - \alpha_{2n}^2)} \left( \alpha_{1n} e^{-\alpha_{1n} x} - \alpha_{2n} e^{-\alpha_{2n} x} \right) \quad \text{for } n > N_c \quad (69)$$

The above expressions are also valid for the antisymmetric case if  $\bar{q}_n(o)$  is replaced by  $\bar{q}_n(o)$  (refer to pages 8 and 9). Values for  $\bar{v}_n$  are given directly by equation (41), while values for  $\bar{u}_n$  can be obtained by substituting equation (42) into equation (39).

### Internal Load Harmonic Coefficients

Values of internal loads in the loaded frame are separated into two parts: one part due to the applied concentrated loads plus the net shear flow components for  $n = 0$  and  $n = 1$ ; the other part due to the net shear flow components for  $n \geq 2$ . This separation is illustrated symbolically for the symmetric case below.

$$\begin{aligned}
 & \text{Circle with } P_o \text{ and curved arrows} = \text{Circle with } P_o \text{ and curved arrows} + \text{Circle with curved arrows} \\
 & -\Delta q = \frac{P_o}{\pi r} \sin \phi \quad -\Delta q = -\sum_{n=2}^{\infty} 2\bar{q}_n(o) \sin n\phi
 \end{aligned}$$

The solution for the first set of loads will be referred to as the "elementary beam theory" part. This solution is well-known and is given on page 24. The part of the solution referred to as the self-equilibrating part is that for which harmonic coefficients can be defined and evaluated simply.

The applied loads do not enter explicitly into the determination of the self-equilibrating part of internal frame loads (only the shear flow). Hence, for properly defined harmonic coefficients, expressions for symmetric and antisymmetric coefficients have identical form. By analogy with the definitions of equations (13) and (14), define:

Symmetric Case	Antisymmetric Case
$\left. \begin{aligned} S &= \sum_{n=2}^{\infty} \bar{S}_n \sin n\phi \\ F &= \sum_{n=2}^{\infty} \bar{F}_n \cos n\phi \\ M &= \sum_{n=2}^{\infty} \bar{M}_n \cos n\phi \end{aligned} \right\} (70)$	$\left. \begin{aligned} S &= - \sum_{n=2}^{\infty} \bar{S}_n \cos n\phi \\ F &= \sum_{n=2}^{\infty} \bar{F}_n \sin n\phi \\ M &= \sum_{n=2}^{\infty} \bar{M}_n \sin n\phi \end{aligned} \right\} (71)$

$\bar{S}_n$ ,  $\bar{F}_n$ ,  $\bar{M}_n$  can be evaluated by substituting the expressions of equation (70) into equations (50), (51) and (52), with  $t_a$ ,  $p_a$ , and  $m_a$  set equal to zero. The results, including the antisymmetric case, are:

$$\left. \begin{aligned} \bar{S}_n &= - \frac{2r}{(1-n^2)} \bar{q}_n(o) \\ \bar{\bar{S}}_n &= - \frac{2r}{(1-n^2)} \bar{\bar{q}}_n(o) \end{aligned} \right\} (72)$$

$$\left. \begin{aligned} \bar{F}_n &= \frac{2rn}{(1-n^2)} \bar{q}_n(o) \\ \bar{\bar{F}}_n &= \frac{2rn}{(1-n^2)} \bar{\bar{q}}_n(o) \end{aligned} \right\} (73)$$

$$\left. \begin{aligned} \bar{M}_n &= \frac{2r^2}{n(1-n^2)} \bar{q}_n(o) \\ \bar{\bar{M}}_n &= \frac{2r^2}{n(1-n^2)} \bar{\bar{q}}_n(o) \end{aligned} \right\} (74)$$

It is noteworthy that the Fourier series for  $S$ ,  $F$ , and  $M$  converge much more rapidly than the series for  $\bar{q}_n(o)$  and  $\bar{\bar{q}}_n(o)$ .

## Displacement Harmonic Coefficients

The radial, tangential, and rotational displacements of the frame are divided into "elementary beam theory" and "self-equilibrating" parts in a slightly different way. If those displacements are expanded in Fourier series, the terms of order  $n = 0$  and  $n = 1$  represent rigid rotation and translation of the frame. The amount of such rigid displacement depends, furthermore, on the manner in which loads are reacted and can be calculated in simple manner from "elementary beam theory." The terms of order  $n \geq 2$  correspond to distortion of the frame. The tangential displacement harmonic coefficients are expressed by equation (49), repeated below, in terms of the shear flow harmonic coefficients.

$$\begin{Bmatrix} \bar{v}_n(o) \\ \bar{\bar{v}}_n(o) \end{Bmatrix} = \frac{r^4}{Ei(n^3 - n)^2} \cdot \frac{K_n}{L_c} \begin{Bmatrix} \bar{q}_n(o) \\ \bar{\bar{q}}_n(o) \end{Bmatrix} \quad \text{for } n \geq 2 \quad (49)$$

The radial and rotational harmonic coefficients are defined as follows:

Symmetric Case	Antisymmetric Case
$\left. \begin{aligned} w &= \sum_{n=2}^{\infty} \bar{w}_n \cos n\phi \\ \theta &= \sum_{n=2}^{\infty} \bar{\theta}_n \sin n\phi \\ v &= \sum_{n=2}^{\infty} \bar{v}_n \sin n\phi \end{aligned} \right\} \quad (75)$	$\left. \begin{aligned} w &= \sum_{n=2}^{\infty} \bar{\bar{w}}_n \sin n\phi \\ \theta &= -\sum_{n=2}^{\infty} \bar{\bar{\theta}}_n \cos n\phi \\ v &= -\sum_{n=2}^{\infty} \bar{\bar{v}}_n \cos n\phi \end{aligned} \right\} \quad (76)$

Substitute equation (75) into equations (54) and (55) and solve for  $\bar{\theta}_n$  and  $\bar{w}_n$  in terms of  $\bar{v}_n$ :

$$\begin{aligned} \bar{w}_n &= n\bar{v}_n \\ \bar{\theta}_n &= \frac{(1 - n^2)}{r} \bar{v}_n \end{aligned} \quad (77)$$

Substitute for  $\bar{v}_n$  from equation (49) and repeat for the antisymmetric case:

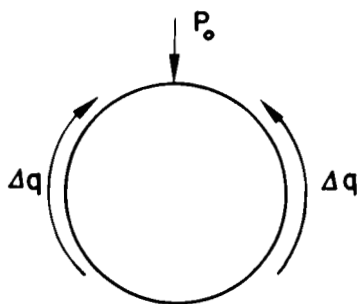
$$\begin{Bmatrix} \bar{w}_n \\ \bar{\bar{w}}_n \end{Bmatrix} = \frac{nr^4}{Ei(n^3 - n)^2} \cdot \frac{K_n}{L_c} \begin{Bmatrix} \bar{q}_n(o) \\ \bar{\bar{q}}_n(o) \end{Bmatrix} \quad (78)$$

$$\begin{Bmatrix} \bar{\theta}_n \\ \bar{\bar{\theta}}_n \end{Bmatrix} = \frac{(1 - n^2)r^3}{Ei(n^3 - n)^2} \cdot \frac{K_n}{L_c} \begin{Bmatrix} \bar{q}_n(o) \\ \bar{\bar{q}}_n(o) \end{Bmatrix} \quad (79)$$

# "Elementary Beam Theory" Part of the Solution

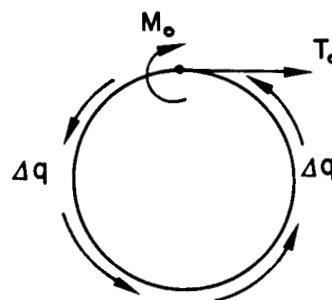
In this section, solutions are written down for the internal loads in the loaded frame due to the external loads shown in figure below.

SYMMETRIC CASE



$$\Delta q = \frac{P_o}{\pi r} \sin \phi$$

ANTISYMMETRIC CASE



$$\Delta q = \frac{1}{2\pi r} \left( T_o + \frac{M_o}{r} \right) + \frac{1}{\pi r} T_o \sin \phi$$

The complete solutions for internal loads are given as reference 3 and reproduced below:

Load	M	S	F
$P_o$	$\frac{P_o r}{2\pi} \left[ 1 + \frac{\cos \phi}{2} - (\pi - \phi) \sin \phi \right]$	$\frac{P_o}{2\pi} \left[ \frac{\sin \phi}{2} - (\pi - \phi) \cos \phi \right]$	$-\frac{P_o}{2\pi} \left[ \frac{3 \cos \phi}{2} + (\pi - \phi) \sin \phi \right]$
$T_o$	$\frac{T_o r}{2\pi} \left[ (\pi - \phi)(1 - \cos \phi) - \frac{3}{2} \sin \phi \right]$	$\frac{T_o}{2\pi} \left[ (\pi - \phi) \sin \phi - \frac{\cos \phi}{2} - 1 \right]$	$\frac{T_o}{2\pi} \left[ \frac{\sin \phi}{2} - (\pi - \phi) \cos \phi \right]$
$M_o$	$\frac{M_o}{2\pi} \left[ (\pi - \phi) - 2 \sin \phi \right]$	$-\frac{M_o}{2\pi r} \left[ 1 + 2 \cos \phi \right]$	$-\frac{M_o}{\pi r} \sin \phi$



## Complete Final Solutions

In this section, all the terms are combined to form complete solutions ready for numerical calculation. In these solutions, the following are not included, as they depend on the location of the reacting loads:

- (1) The "elementary beam theory" part of the shear flow which should be calculated from beam theory.
- (2) The "elementary beam theory" part of axial load intensity ( $p$ ) which should be calculated from beam theory.
- (3) The rigid translation and rotation of the loaded frame.

Shear Flow Harmonic Coefficients

$$\text{Symmetric: } \bar{q}_n(o) = \frac{\frac{n}{2\pi r} P_o}{1 + \gamma K_n} \quad (66)$$

$$\text{Antisymmetric: } \bar{\bar{q}}_n(o) = \frac{-\frac{1}{2\pi r} \left[ T_o + \frac{(1-n^2)}{r} M_o \right]}{1 + \gamma K_n} \quad (67)$$

Shear Flow

$$q = \sum_{n=2}^{n < N_c} \left[ \bar{q}_n(o) \sin n\phi - \bar{\bar{q}}_n(o) \cos n\phi \right] e^{-\alpha_n x} \left\{ \cos \beta_n x - \frac{(\alpha_n^2 - \beta_n^2)}{2\alpha_n \beta_n} \sin \beta_n x \right\} \\ + \sum_{n > N_c}^{\infty} \left[ \bar{q}_n(o) \sin n\phi - \bar{\bar{q}}_n(o) \cos n\phi \right] \left\{ \frac{\alpha_{1n}^2 e^{-\alpha_{1n} x} - \alpha_{2n}^2 e^{-\alpha_{2n} x}}{\alpha_{1n}^2 - \alpha_{2n}^2} \right\} \quad (80)$$

Axial Load in Effective Skin of Thickness  $t'$ 

$$p = \sum_{n=2}^{n < N_c} \left[ -\bar{q}_n(o) \cos n\phi - \bar{\bar{q}}_n(o) \sin n\phi \right] \left\{ \frac{n e^{-\alpha_n x}}{2r \alpha_n} \left( \cos \beta_n x - \frac{\alpha_n}{\beta_n} \sin \beta_n x \right) \right\} \\ + \sum_{n > N_c}^{\infty} \left[ -\bar{q}_n(o) \cos n\phi - \bar{\bar{q}}_n(o) \sin n\phi \right] \left\{ \frac{n}{r} \left( \frac{\alpha_{1n} e^{-\alpha_{1n} x} - \alpha_{2n} e^{-\alpha_{2n} x}}{\alpha_{1n}^2 - \alpha_{2n}^2} \right) \right\} \quad (81)$$

Frame Bending Moment

M = "elementary beam theory" part given in table on page 23

$$+ \sum_{n=2}^{\infty} \left[ \bar{q}_n(o) \cos n\phi + \bar{\bar{q}}_n(o) \sin n\phi \right] \frac{2r^2}{n(1-n^2)} \quad (82)$$

Frame Shear

S = "elementary beam theory" part given in table on page 23

$$+ \sum_{n=2}^{\infty} \left[ -\bar{q}_n(o) \sin n\phi + \bar{\bar{q}}_n(o) \cos n\phi \right] \frac{2r}{(1-n^2)} \quad (83)$$

Frame Axial Load

F = "elementary beam theory" part given in table on page 23

$$+ \sum_{n=2}^{\infty} \left[ \bar{q}_n(o) \cos n\phi + \bar{\bar{q}}_n(o) \sin n\phi \right] \frac{2rn}{(1-n^2)} \quad (84)$$

Frame Tangential Displacement

$$v = \sum_{n=2}^{\infty} \left[ \bar{q}_n(o) \sin n\phi - \bar{\bar{q}}_n(o) \cos n\phi \right] \frac{2r^4}{EI_o} \cdot \frac{\gamma K_n}{(n^3 - n)^2} \quad (85)$$

Frame Radial Displacement

$$w = \sum_{n=2}^{\infty} \left[ \bar{q}_n(o) \cos n\phi + \bar{\bar{q}}_n(o) \sin n\phi \right] \frac{2r^4}{EI_o} \cdot \frac{n \gamma K_n}{(n^3 - n)^2} \quad (86)$$

Frame Rotation

$$\theta = \sum_{n=2}^{\infty} \left[ \bar{q}_n(o) \sin n\phi - \bar{\bar{q}}_n(o) \cos n\phi \right] \frac{2r^3}{EI_o} \cdot \frac{(1-n^2) \gamma K_n}{(n^3 - n)^2} \quad (87)$$

Numerical Computations

Equations (80) to (87) have been evaluated using an IBM 704 computer. Twenty terms of the Fourier series were used, and tables, giving the coefficients  $C_{ik}$  defined below,

are included in reference 7 for  $L_r/L_c = 0.2, 0.4, \text{ and } 1.0$ .

$$q = C_{qp} \frac{P_o}{r} + C_{qt} \frac{T_o}{r} + C_{qm} \frac{M_o}{r^2} \quad (88)$$

$$p = C_{pp} \frac{P_o}{r} \left( \frac{L_c}{r} \right) + C_{pt} \frac{T_o}{r} \left( \frac{L_c}{r} \right) + C_{pm} \left( \frac{M_o}{r^2} \right) \frac{L_c}{r} \quad (89)$$

$$M = C_{mp} P_o r + C_{mt} T_o r + C_{mm} M_o \quad (90)$$

$$S = C_{sp} P_o + C_{st} T_o + C_{sm} \frac{M_o}{r} \quad (91)$$

$$F = C_{fp} P_o + C_{ft} T_o + C_{fm} \frac{M_o}{r} \quad (92)$$

$$v = C_{vp} P_o \frac{\gamma r^3}{EI_o} + C_{vt} T_o \frac{\gamma r^3}{EI_o} + C_{vm} M_o \cdot \frac{\gamma r^2}{EI_o} \quad (93)$$

$$w = C_{wp} P_o \frac{\gamma r^3}{EI_o} + C_{wt} T_o \frac{\gamma r^3}{EI_o} + C_{wm} M_o \cdot \frac{\gamma r^2}{EI_o} \quad (94)$$

$$\theta = C_{\theta p} P_o \frac{\gamma r^2}{EI_o} + C_{\theta t} T_o \frac{\gamma r^2}{EI_o} + C_{\theta m} M_o \frac{\gamma r}{EI_o} \quad (95)$$

#### Illustration of the Effect of Frame Flexibility on Shell Loads

To illustrate the application of the solutions to a practical problem, consider the stress analysis of a transport airplane fuselage with the characteristics given below and subjected to an inward-acting radial load of 10,000 lbs at a frame whose moment of inertia is  $2.0 \text{ in.}^4$ . It is well known that the stresses in the loaded frame are considerably different from those derived by the use of beam theory and they are not discussed here. They can be obtained from any of references 1, 4, or 7. Instead, attention is focussed on the stresses in the shell.

##### Structural Characteristics

$$I_o = 2.0 \text{ in.}^4$$

$$t = 0.04 \text{ in.}$$

$$P_o = 10,000 \text{ lbs}$$

$$I = 0.5 \text{ in.}^4$$

$$t' = 0.20 \text{ in.}$$

$$\ell_o = 15.0 \text{ in.}$$

$$r = 60.0 \text{ in.}$$

Parameters required are calculated from the above.

$$L_c = 300 \text{ in.} \quad L_r = 115 \text{ in.} \quad L_r / L_c = 0.385, \underline{a} 0.40 \quad \gamma = 0.10$$

Using these parameters in the tables of reference 7 and equations (88) and (89) provides the information necessary to plot figures 5 and 6. The plotted shear flows (and stresses) and axial load intensities (and stresses) are corrections to "elementary beam theory" only (see page 24).

In the stress analysis of cylindrical shells supported by frames it is common practice to account for a departure from "elementary beam theory" of the shear stresses in the immediate vicinity of the frame. Figure 5 shows that the perturbation in shear flows propagates considerably farther in the axial direction than is normally allowed for in the design. At one value of  $\phi$ , sixty inches away from the loaded frame, the shear stress differs from that predicted by "elementary beam theory" by 1500 lbs/in<sup>2</sup>.

The differences in the axial stresses predicted by "elementary beam theory" and the method of this report are even more marked. The beam theory suggests zero axial stress in the shell at the station of the externally-loaded frame, while this report gives 3125 lbs/in<sup>2</sup> (see figure 6).

Lockheed Aircraft Corporation,  
California Division,  
Burbank, Calif., October 1959.

L-1028

## APPENDIX A

### CORRECTION FOR FINITE FRAME SPACING

In the main text, "A Reinforced Loaded Frame in an Infinite, Uniform Shell," solutions are obtained for an idealized shell whose unloaded frames are "smeared out" in the axial direction to produce a uniform bending rigidity  $Ei$  per unit length. To account for the effects of finite frame spacing there are two alternatives. One is to write the equations for a finite length of shell in which  $i$  is put equal to the circumferential bending stiffness per unit length of the skin-stringer combination, and use the exact methods indicated in reference 6; however, such a solution would either have to be derived for each particular combination of shell and frame characteristics or more parameters would have to be introduced and the number of tables of the type included in reference 7 would increase greatly. The second alternative is far more expedient; it is to consider a technique whereby a correction to the basic parameter  $\gamma$  is computed. As a result, the first section and the tables of reference 7 can be used. To accomplish this, the problem of a "frameless" bay adjacent to the loaded frame in an infinite shell is solved exactly and used to derive approximate corrections to the solutions of the first section. A comparison is made with the solutions of reference 4 for a shell with equally spaced frames to check the validity of these approximate corrections.

Distributing the frames in the axial direction, to give the shell a continuously distributed bending stiffness, has two main effects on the stress distribution near the loaded frame. These are:

- (1) Since the loaded frame is not "smeared out", bending stiffness of  $i \ell_o / 2$  is effectively added to the shell on either side of the loaded frame.
- (2) Since the cross section undergoes more distortion near the loaded frame than it does at a distance, the shell with "smeared-out" frames offers additional support over and above that included in (1).

If the frame spacing is small, compared to the characteristic length, and if the loaded frame is heavily reinforced, the effect of finite frame spacing is small. A criterion for estimating the importance of the effect is the following:

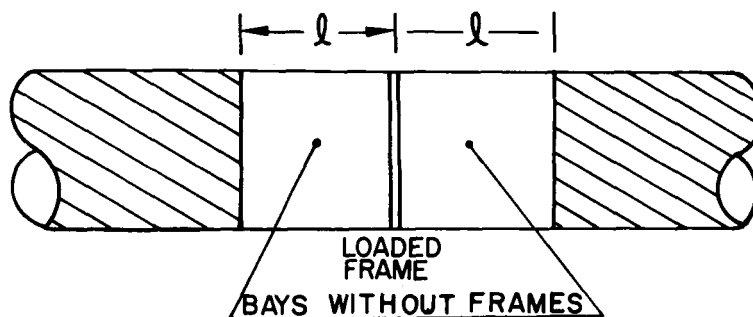
For

$$\frac{I_o}{I} \cdot \frac{L_c}{\ell_o} = 2\gamma \left( \frac{L_c}{\ell_o} \right)^2 \geq 50 \quad (A.1)$$

the effect of finite frame spacing on stresses in the loaded frame is negligible.

The "smearing out" of frames, other than ones immediately adjacent to the loaded frame, has little effect on stresses in the loaded frame. Consequently, the effect of neglecting finite frame spacing can be approximated by including

a bay on either side of the loaded frame which has no bending stiffness, as shown below.



The value of  $l$  selected for the above representation should be greater than  $l_0/2$  and less than  $l_0$ . For  $l = l_0/2$ , the shell has correct total bending stiffness but the distance from the loaded frame to the first supporting shell-bending element is smaller by a factor of 2 than in the actual structure. For  $l = l_0$ , this distance is correct, but the total bending stiffness of the shell is too small by an amount,  $il_0$ . In one example worked out later, it is shown that  $l = 3/4 l_0$  gives good results.

The effect of finite frame spacing introduces an additional parameter,  $l_0/L_c$ , into the problem. This is undesirable from the point of view of computations, since it increases the number of charts or tables that must be prepared. Consequently, an attempt is made to account for finite frame spacing by modifying the "beef-up" parameter,  $\gamma$ .

The solutions given in reference 4 are correct for a shell with equally-spaced, concentrated frames that have equal bending stiffness (including the loaded frame). Hence, the approximations considered here can be evaluated by comparison of these results with the results given in reference 4. The assumption in reference 4 that the loaded frame has the same moment of inertia as unloaded frames gives very low values to the quantity on the left side of equation (A-1), which quantity has been suggested as a criterion for the importance of finite frame spacing. It is shown that reasonably good agreement is obtained between the results obtained by the approximations and the results given in reference 4, so the approximations can be applied with confidence to other cases.

### Characteristics of a Bay Without Frames

The differential equations for a shell without circumferential bending stiffness can be obtained from equations (16) to (19) of the first section by setting  $i = 0$  in equation (16). The results for symmetrical harmonic coefficients are:

$$\frac{d\bar{q}_n}{dx} = 0 \quad (A. 2)$$

$$\frac{d\bar{p}_n}{dx} - \frac{n}{r} \bar{q}_n = 0 \quad (A. 3)$$

$$\bar{p}_n = Et' \frac{d\bar{u}_n}{dx} \quad (A. 4)$$

$$\bar{q}_n = Gt \left[ \frac{n}{r} \bar{u}_n - \frac{d\bar{v}_n}{dx} \right] \quad (A. 5)$$

The general solution of these equations is:

$$\bar{q}_n = \bar{q}_n(o) \quad (A. 6)$$

$$\bar{p}_n = \frac{nx}{r} \bar{q}_n(o) + \bar{p}_n(o) \quad (A. 7)$$

$$\bar{u}_n = \frac{1}{2} \cdot \frac{nx^2}{Et' r} \bar{q}_n(o) + \frac{x}{Et'} \bar{p}_n(o) + \bar{u}_n(o) \quad (A. 8)$$

$$\begin{aligned} \bar{v}_n = & \left[ \frac{n^2 x^3}{6 Et' r^2} - \frac{x}{Gt} \right] \bar{q}_n(o) + \frac{nx^2}{2Et' r} \bar{p}_n(o) \\ & + \frac{nx}{r} \bar{u}_n(o) + \bar{v}_n(o) \end{aligned} \quad (A. 9)$$

In the present example,  $\bar{u}_n(o) = 0$ , since distortions of the shell are symmetrical with respect to the plane of the loaded frame,  $x = 0$ . Evaluate equations (A. 8) and (A. 9) at  $x = \ell$  with  $\bar{u}_n(o) = 0$ . Then eliminate  $\bar{p}_n(o)$ ,  $\bar{q}_n(o)$  by use of equations (A. 6) and (A. 7). This leads to:

$$\bar{v}_n(\ell) = \bar{v}_n(o) - D_{11} \bar{q}_n(\ell) + D_{12} \bar{p}_n(\ell) \quad (A. 10)$$

$$\bar{u}_n(\ell) = -D_{21} \bar{q}_n(\ell) + D_{22} \bar{p}_n(\ell) \quad (A. 11)$$

where

$$D_{11} = \left[ \frac{\ell}{Gt} + \frac{n^2 \ell^3}{3Et' r^2} \right]$$

$$D_{12} = D_{21} = \frac{n\ell^2}{2Et' r} \quad D_{22} = \frac{\ell}{Et'}$$

#### General Solution for Shell with Frameless Bays Adjacent to the Loaded Frame

Additional relationships between  $\bar{q}_n(\ell)$ ,  $\bar{p}_n(\ell)$ ,  $\bar{u}_n(\ell)$  and  $\bar{v}_n(\ell)$  are obtained from the equations for the shell with "smeared-out" frames extending from  $x = \ell$  to infinity. These relationships are derived in Appendix B, and may be written:

$$\bar{v}_n(\ell) = Z_{11} \bar{q}_n(\ell) + Z_{12} \bar{p}_n(\ell) \quad (A.12)$$

$$\bar{u}_n(\ell) = Z_{21} \bar{q}_n(\ell) + Z_{22} \bar{p}_n(\ell) \quad (A.13)$$

where

$$Z_{11} = \frac{36 L_c^3}{Et' r^2 n^2 (n^2 - 1)^2} \cdot 2 \alpha_n L_c$$

$$Z_{12} = -Z_{21} = \frac{6 L_c^2}{Et' r n (n^2 - 1)}$$

$$Z_{22} = -12 L_c \alpha_n / Et' n^2 (n^2 - 1)$$

Eliminate  $\bar{u}_n(\ell)$  and  $\bar{v}_n(\ell)$  from equations (A.10), (A.11), (A.12) and (A.13).

$$\bar{v}_n(o) = (Z_{11} + D_{11}) \bar{q}_n(\ell) + (Z_{12} - D_{12}) \bar{p}_n(\ell) \quad (A.14)$$

$$0 = (Z_{21} + D_{21}) \bar{q}_n(\ell) + (Z_{22} - D_{22}) \bar{p}_n(\ell) \quad (A.15)$$

Replace  $\bar{q}_n(\ell)$  by  $\bar{q}_n(o)$  from equation (A.6) and solve for  $\bar{v}_n(o) / \bar{q}_n(o)$ :

$$\frac{\bar{v}_n(o)}{\bar{q}_n(o)} = (Z_{11} + D_{11}) - \frac{(Z_{12} - D_{12})(Z_{21} + D_{21})}{(Z_{22} - D_{22})} \quad (A.16)$$



This expression replaces equation (49) for the problem at hand. The solution from this point on is identical with the solution given in the main text. Equation (49) can be written as:

$$\frac{\bar{v}_n(0)}{\bar{q}_n(0)} = \frac{36 L_c^3 K_n}{n^2 (n^2 - 1)^2 Et' r^2} \quad (A. 17)$$

$K_n$  is the only factor which enters the solution in the main text. Hence, let the solution for the present case be given by:

$$\frac{\bar{v}_n(0)}{\bar{q}_n(0)} = \frac{36 L_c^3 \bar{K}_n(\ell)}{n^2 (n^2 - 1)^2 Et' r^2} \quad (A. 18)$$

where

$$\bar{K}_n(\ell) = \frac{n^2 (n^2 - 1)^2 Et' r^2}{36 L_c^3} \left[ (Z_{11} + D_{11}) - \frac{(Z_{12} - D_{12})(Z_{21} + D_{21})}{(Z_{22} - D_{22})} \right] \quad (A. 19)$$

Further development of the solution can be confined to the evaluation of  $\bar{K}_n(\ell)$ .

For  $\ell = 0$ ,  $\bar{K}_n$  must be equal to  $K_n$ . For  $\ell = 0$ ,  $D_{11}$ ,  $D_{12}$ ,  $D_{21}$ , and  $D_{22}$  vanish.

Hence,

$$\bar{K}_n(0) = \frac{n^2 (n^2 - 1)^2 Et' r^2}{36 L_c^3} \left[ Z_{11} - \frac{Z_{12} Z_{21}}{Z_{22}} \right] \quad (A. 20)$$

This equality may be verified by direct substitution for  $Z_{11}$ ,  $Z_{12}$ ,  $Z_{21}$ , and  $Z_{22}$ , and compared with the defining formula for  $K_n$  in equation (46). Equation (A. 19) may be rewritten as follows to incorporate the result of equation (A. 20).

$$\bar{K}_n(\ell) = K_n + \frac{(n^3 - n)^2 Et' r^2}{36 L_c^3} \left[ D_{11} + \frac{Z_{12} Z_{21}}{Z_{22}} - \frac{(Z_{12} - D_{12})(Z_{21} + D_{21})}{(Z_{22} - D_{22})} \right] \quad (A. 21)$$

Substitute explicit values for letter symbols and obtain after some algebraic manipulation and introduction of the parameters,  $L_r$  and  $a_n$ ,

$$\bar{K}_n(\ell) = K_n + \frac{(n^3 - n)^2}{36} \left( \frac{\ell}{L_c} \right) \left[ 4 \left( \frac{L_r}{L_c} \right)^2 + \frac{n}{3} \left( \frac{\ell}{L_c} \right)^2 + \frac{3 \left( 1 + 2 \alpha_n \ell - \frac{\alpha_n^3 \ell^3}{1 + a_n} \right)}{(n^2 - 1)(1 + a_n + \alpha_n \ell)} \right] \quad (A. 22)$$

This expression can be used in place of  $K_n$  in the results of the main text, in order to get an accurate solution of the substitute problem.

### Approximate Corrections for Finite Frame Spacing

If it is assumed that  $\ell/L_c$  is small and that terms for large value of  $n$  are unimportant, a reasonably accurate approximation to equation (A. 22) is obtained by omitting terms in  $\ell^2$ ,  $\ell^3$ , etc. This gives

$$\bar{K}_n(\ell) = K_n + \frac{(n^3 - n)^2}{36} \left( \frac{\ell}{L_c} \right) \left[ 4 \left( \frac{L_r}{L_c} \right)^2 + \frac{3}{(n^2 - 1)(1 + a_n)} \right] \quad (A. 23)$$

which reduces to:

$$\bar{K}_n(\ell) = K_n + \frac{\ell}{L_c} (K_n^0)^2 \left[ 4 a_n + \frac{1}{1 + a_n} \right] \quad (A. 24)$$

where  $K_n^0 = \frac{n\sqrt{n^2 - 1}}{2\sqrt{3}}$  and is the value of  $K_n$  for  $\frac{L_r}{L_c} = 0$ .

Since  $K_n$  enters into calculations multiplied by  $\gamma$  [see equations (66) and (67)] it is useful to consider the change in  $K_n$  as an equivalent change in  $\gamma$ . Let

$$\gamma \bar{K}_n(\ell) = \gamma_{\ell, n} \cdot K_n$$

where

$$\gamma_{\ell, n} = \gamma \left[ 1 + \frac{\ell}{L_c} \frac{(K_n^0)^2}{K_n} \left( 4 a_n + \frac{1}{1 + a_n} \right) \right] \quad (A. 25)$$

For large value of  $n$ ,  $\gamma_{\ell, n}$  increases as  $n^2$  for  $L_r/L_c = 0$ , and as  $n^3$  for  $L_r/L_c > 0$ .

For  $n = 2$  and  $L_r/L_c = 0$

$$\gamma_{\ell, 2} = \gamma \left( 1 + \frac{\ell}{L_c} \right) \quad (A. 26)$$

To treat the dependence of  $\gamma_{\ell, n}$  on  $n$  correctly,  $\ell/L_c$  must be introduced into the solution as a separate parameter. In order to avoid this difficulty,  $\gamma_{\ell, n}$  may be replaced by an approximate constant,  $\gamma^*$ , chosen to give a best fit to the family of values of  $\gamma_{\ell, n}$ . Considerations pertinent to the choice of this constant are:

- (1) For large values of  $\gamma$  (heavy reinforced frame) the term for  $n = 2$  dominates in the solution.

(2) The choice of  $\ell$  in equation (A. 25) should not be less than  $\ell_0/2$ .

(3)  $\gamma_{\ell, n}$  increases as  $n^2$  or  $n^3$ .

In view of these considerations, for large values of  $\gamma$  let:

$$\gamma^* = \gamma \left[ 1 + \frac{\ell_0 (K_2^0)^2}{2 L_c K_2} \left( 4 a_2 + \frac{1}{1 + a_n} \right) \right] \quad (\text{A. 27})$$

For smaller values of  $\gamma K_2$ ,  $\gamma^*$  should be smaller than indicated by equation (A. 27). An empirical rule that will be shown to be satisfactory is:

$$\gamma^* = \gamma \left[ 1 + \frac{\ell_0}{2 L_c} \cdot \frac{\sqrt{1 + (L_r/L_c)^2}}{1 + 2 (L_r/L_c)^2} \cdot \left( 1 + \frac{1}{2 \gamma K_2} \right) \left\{ 4 \left( \frac{L_r}{L_c} \right)^2 + \frac{1}{1 + (L_r/L_c)^2} \right\} \right] \quad (\text{A. 28})$$

where the substitution  $a_2 = (L_r/L_c)^2$  has been made. The following table shows the value of  $\gamma$  for which values of  $\gamma_{\ell, n}$  and  $\gamma^*$  are equal, assuming  $\ell = \ell_0/2$  and  $L_r/L_c = 0$ .

n	$\gamma$
2	$\infty$
3	.345
4	.144
5	.082

The rule given in equation (A. 28) makes it possible to introduce a correction for finite frame spacing by modifying the value of  $\gamma$ .

By using the concordance established between the parameters of this report and those of reference 4, it is possible to compare the results of the two solutions. The required relationships are developed in Appendix C. Values of the parameters were chosen to represent the extreme ranges in airplane fuselage construction and a number of curves were plotted, using equation (A. 28) to correct the beef-up parameter for the effects of finite frame spacing. In all cases, the value of the criterion of equation (A. 1) was small and hence, the correction to  $\gamma$  was substantial. A typical example is shown in figure 7 in which the effects of the accurate and approximate corrections [equations (A. 24) and (A. 28), respectively,] can be compared. The correction for finite frame spacing, suggested in equation (A. 28), is considered satisfactory.

Correction to the Example of "Illustration of the Effect of Frame Flexibility on Shell Loads" (page 26)

Substituting the parameters of the example into equation (A. 28) gives a value for  $\gamma^*$  of 0.13. Corrections of this order of magnitude produce small changes in the stresses computed, using  $\gamma = 0.10$ .

## APPENDIX B

### REINFORCED LOADED FRAME AT FREE END OF A SEMI-INFINITE UNIFORM CYLINDRICAL SHELL

#### Statement of the Problem

It is convenient at this stage to consider the case of a loaded frame at the free end of a semi-infinite shell. The solution to this problem is required when solving problems concerned with a shell that is non-uniform in the axial direction.\* In particular, the Input Impedance is required.

#### Solution

The differences between the solution of this problem and that of the infinite shell are due to the boundary conditions at  $x = 0$ . For the semi-infinite shell there is zero direct stress in the shell at  $x = 0$ , while in the infinite shell, axial extension is prevented at  $x = 0$ , due to symmetry.

It is shown in the main text that the Input Impedance to an infinite shell is the same for  $n < N_c$  as it is for  $n > N_c$ . Here the case of  $n < N_c$  is computed, corresponding to characteristic equation of the general solution having complex roots.

The general solution for an applied radial load is:

$$\begin{pmatrix} \bar{p}_n \\ \bar{q}_n \\ \bar{u}_n \\ \bar{v}_n \end{pmatrix} = e^{-\alpha_n x} \left[ \begin{pmatrix} E_{pn} \\ E_{qn} \\ E_{un} \\ E_{vn} \end{pmatrix} \sin \beta_n x + \begin{pmatrix} \bar{p}_n(0) \\ \bar{q}_n(0) \\ \bar{u}_n(0) \\ \bar{v}_n(0) \end{pmatrix} \cos \beta_n x \right] \quad (B.1)$$

The equations for applied antisymmetric loads take exactly the same form, and what follows applies to them also.

\* See reference 6 and the correction for finite frame spacing in Appendix A.

From equation (B.1) we have

$$\frac{d\bar{p}_n}{dx} = e^{-\alpha_n x} \left[ - \left\{ \alpha_n E_{pn} + \beta_n \bar{p}_n(o) \right\} \sin \beta_n x + \left\{ \beta_n E_{pn} - \alpha_n \bar{p}_n(o) \right\} \cos \beta_n x \right] \quad (B.2)$$

and similar expressions for  $\frac{d\bar{q}_n}{dx}$ ,  $\frac{d\bar{u}_n}{dx}$  and  $\frac{d\bar{v}_n}{dx}$ .

The eight constants in equation (B.1) can be evaluated by the use of equations (16) to (19), of which only three of the four equations (16), (17), (18), and (19) are independent. Equations (16), (17) and (18) are used. The coefficients of the Sine terms must be equal and likewise the coefficients of the Cosine terms. Substituting equation (B.1) into equation (16), we have, equating first the coefficients of Sine terms and then Cosine terms,

$$\left. \begin{aligned} \alpha_n E_{qn} + \beta_n \bar{q}_n(o) &= \frac{Ei}{r^4} (n^3 - n)^2 E_{vn} \\ - \beta_n E_{qn} + \alpha_n \bar{q}_n(o) &= \frac{Ei}{r^4} (n^3 - n)^2 \bar{v}_n(o) \end{aligned} \right\} \quad (B.3)$$

Substituting equation (B.1) into equation (17) and equating coefficients leads to:

$$\left. \begin{aligned} - \alpha_n E_{pn} - \beta_n \bar{p}_n(o) &= \frac{n}{r} E_{qn} \\ \beta_n E_{pn} - \alpha_n \bar{p}_n(o) &= \frac{n}{r} \bar{q}_n(o) \end{aligned} \right\} \quad (B.4)$$

Similarly, substituting equation (B.1) into equation (18) gives

$$\left. \begin{aligned} - \alpha_n E_{un} - \beta_n \bar{u}_n(o) &= \frac{1}{Et} E_{pn} \\ \beta_n E_{un} - \alpha_n \bar{u}_n(o) &= \frac{1}{Et} \bar{p}_n(o) \end{aligned} \right\} \quad (B.5)$$

Eliminating  $E_{pn}$ ,  $E_{qn}$ ,  $E_{un}$ , and  $E_{vn}$  from equations (B.3), (B.4) and (B.5), the following two equations are derived:

$$\left| \begin{array}{l} v_n(o) \\ u_n(o) \end{array} \right| = \left[ \begin{array}{l} \frac{2\alpha_n r^4}{Ei(n^3 - n)^2} + \frac{r}{n} (\alpha_n^2 + \beta_n^2) \frac{r^4}{Ei(n^3 - n)^2} \\ - \frac{n}{r} \cdot \frac{1}{Et(\alpha_n^2 + \beta_n^2)} - \frac{2\alpha_n}{Et(\alpha_n^2 + \beta_n^2)} \end{array} \right] \left| \begin{array}{l} q_n(o) \\ p_n(o) \end{array} \right|$$

Introducing the relationships for the characteristic lengths gives

$$\begin{vmatrix} \bar{v}_n(o) \\ \bar{u}_n(o) \end{vmatrix} = \frac{6L_c}{Et' n^2(n^2 - 1)} \begin{bmatrix} \frac{12 L_c^3 \alpha_n}{r^2(n^2 - 1)} + \frac{nL_c}{r} \\ -\frac{nL_c}{r} - 2\alpha_n L_c \end{bmatrix} \begin{vmatrix} \bar{q}_n(o) \\ \bar{p}_n(o) \end{vmatrix} \quad (B.6)$$

Equations (B.6) are the stress-displacement relationships at the free end of a semi-infinite shell. It should be noted that equations (B.6), derived for  $x = 0$ , hold at any point  $x$ , provided the shell is uniform between  $x$  and  $\infty$ . The equations for antisymmetric applied loadings are of the same form with  $\bar{q}_n(o)$ , replacing  $\bar{q}_n(o)$ , etc. It can be shown that they are true for real roots of the characteristic equation. Equations (B.6) are used in reference 6 in the solution of a practical shell problem.

#### Input Impedance at a Free End

The Input Impedance,  $\bar{v}_n(o)/\bar{q}_n(o) = \bar{\bar{v}}_n(o)/\bar{\bar{q}}_n(o)$ , at a free end is found directly from equations (B.6) by setting  $\bar{p}_n(o) = 0$ .

$$\frac{\bar{v}_n(o)}{\bar{q}_n(o)} = \frac{36}{(n^3 - n)^2} \cdot 2L_c \alpha_n \cdot \frac{L_c^3}{Et' r^2} = \frac{36 L_c^3}{(n^3 - n)^2 Et' r^2} \cdot \frac{n \sqrt{n^2 - 1}}{\sqrt{3}} \sqrt{1 + \frac{(n^2 - 1)}{3} \left(\frac{L_r}{L_c}\right)^2} \quad (B.7)$$

#### Calculation of Harmonic Coefficients

The method follows that method used in the main text. A relationship between shear flow and tangential displacement coefficients in the shell at  $x = 0$  is found in equation (B.7). This relationship is substituted in equation (62) to yield the shear flow harmonic coefficient at  $x = 0$ . From this point a complete solution to the problem, analogous to that for the doubly infinite shell, can be developed by applying the boundary condition  $\bar{p}_n(o) = 0$ , instead of  $\bar{u}_n(o) = 0$ , for the case of the doubly infinite shell, to equations (34) and (35). In what follows only the symmetric loading case is discussed since the results hold for unsymmetric cases, except for expressions involving external loading.

Equation (B.7) can be written, using the relationship  $Et' = 36 Ei L_c^4/r^6$ , as

$$\frac{\bar{v}_n(o)}{\bar{q}_n(o)} = \frac{r^4}{Ei} \cdot \frac{2\alpha_n}{(n^3 - n)^2} \quad (B.8)$$

Substituting equation (B. 8) into equation (62) and noting that since the loaded frame is supported by the shell on one side only,  $\Delta \bar{q}_n = \bar{q}_n(o)$ ,

$$\bar{q}_n(o) = \frac{\frac{n P_o}{\pi r}}{(1 + 4\gamma L_c \alpha_n)} \quad (B. 9)$$

The antisymmetric shear flow coefficient at  $x = 0$  is derived in the same manner as the symmetric coefficient and is:

$$\bar{\bar{q}}_n(o) = \frac{-\frac{1}{\pi r} \left\{ T_o + \frac{(1 - n^2)}{r} M_o \right\}}{(1 + 4\gamma L_c \alpha_n)} \quad (B. 10)$$

Comparison of equation (B. 9) with equation (66), the equivalent equation for the infinite shell, shows they are the same except that  $4L_c \alpha_n$  replaces  $K_n$ .

Now it is a simple matter to derive a complete solution for the stress and displacement distributions for the semi-infinite shell, with loaded frame at free end, as explained above.

## APPENDIX C

### RELATIONSHIPS OF PARAMETERS OF THIS REPORT WITH THOSE OF REFERENCES 1 AND 4

It is important to be able to compare the results of this report with other solutions to the problem of a loaded frame in a circular, cylindrical shell. References 1 and 4 present two such solutions whose derivations are based on assumptions different from those of this report. It is of interest to compare the parameters of the three methods and derive relationships between these parameters.

#### Comparison of Parameters of This Report With Those of Reference 4

In order to compare the results derived in the main text of this report and those of reference 4, a concordance must be established between the parameters of this report and those of reference 4. A direct comparison of the parameters involved shows the following relationships exist:

$$\begin{aligned} \gamma &= \frac{\sqrt{6}}{2A^{1/4}} & \frac{l_o}{L_c} &= \frac{\sqrt{6}}{A^{1/4}} & A &= \frac{2.25}{\gamma^4} \\ \frac{L_r}{L_c} &= \frac{\sqrt{6}}{2} \cdot \frac{A^{1/4}}{\sqrt{A/B}} & & & \frac{A}{B} &= \frac{2.25}{\gamma^2 (L_r/L_c)^2} \end{aligned} \quad (C. 1)$$

$I_0 = i\ell_0$ , due to the assumption of identical frames throughout the shell, in reference 4.

The curves of reference 4 can be used for the analysis of reinforced frames in shells whose frames are not uniformly spaced, by means of equations (C.1). In so doing, the frame spacing,  $\ell_0$ , given by equation (C.1) should be checked with the actual value of frame spacing. If the value in equation (C.1) is much larger than the actual value, the results given by the curves in reference 4 may be inaccurate. This application of reference 4 amounts to relumping the frames so that all the idealized frames have stiffness equal to the stiffness of the loaded frame.

#### Comparison of Parameters of This Report With Those of Reference 1

##### Infinitely Long Uniform Shell

In reference 1, the assumption is made that the tangential displacement of the loaded frame is proportional to the local value of shear flow. The form of this relationship is:

$$\frac{v}{q} = \frac{2L}{Gt} \quad (C.2)$$

where  $Gt$  is the shear stiffness of the skin panel (assumed uniform) and  $L$  is an unspecified length, (except for the recommendation that it should never be made greater than the radius of the shell). In the terminology of this report, the above equation gives,

$$\frac{\bar{v}_n(o)}{\bar{q}_n(o)} = \frac{\bar{v}_n(o)}{\bar{q}_n(o)} = \frac{2L}{Gt} \quad (C.3)$$

$L$  may be evaluated by comparing equations (A.17) and (C.3). One form of the result is:

$$L = L_c \left( \frac{L_c}{L_r} \right)^2 \frac{4.5 K_n}{(n^3 - n)^2} \quad (C.4)$$

Note that  $L$  is a function of  $n$ . In fact, for  $L_r/L_c = 0$ ,  $L$  decreases as  $1/n^4$ ; for  $L_r/L_c > 0$  and  $n$  large,  $L$  decreases as  $1/n^3$ .

Since a constant value of  $L$  has been assumed in reference 1, a direct comparison with the present theory cannot be achieved. A device similar to that employed in the correction for finite frame spacing is required.

The curves presented in reference 1 are drawn as a function of the parameter,  $d$ , defined below:

$$d = \frac{r^4 Gt}{I_0 L E} \quad (C.5)$$



If the value of  $L$  obtained in equation (C.4) is substituted into this definition,

$$d = \frac{(n^3 - n)^2}{\gamma K_n} \quad (C.6)$$

Note that  $d$  is also a function of  $n$ . In fact,  $d$  increases as  $n^4$  for  $L_r/L_c = 0$ , and as  $n^3$  for  $L_r/L_c > 0$  and  $n$  large.

For large values of  $\gamma$  the term for  $n = 2$  dominates the solution. In this case

$$d_2 = \frac{36}{\gamma} \cdot \frac{\sqrt{1 + (L_r/L_c)^2}}{1 + 2(L_r/L_c)^2} \quad (C.7)$$

This analytic expression for  $d$  may be used, in connection with the curves of reference 1, for sufficiently large values of  $\gamma$ .

In order to obtain the limits of applicability of equation (C.7) and an empirical relation between  $d$  and  $\gamma$  for small  $\gamma$ , the following table gives values of  $d$  calculated by equation (C.6) and corresponding to various values of the parameters in reference 4.

TABLE C-1  
VALUES OF  $d$  CORRESPONDING TO VARIOUS  
VALUES OF PARAMETERS A AND A/B IN REFERENCE 4

A	200		$2 \times 10^4$		$2 \times 10^6$	
A/B	$\infty$	30	$\infty$	100	$\infty$	1000
$\gamma$	3.26		.1032		.0326	
$L_r/L_c$	0	.84	0	1.46	0	1.46
$n$	d	d	d	d	d	d
2	110	60	350	117	1,110	372
3	722	258	2780	477	7,220	1,510
4	2460	660	7800	1200	24,600	3,800
5	6240	1260	19700	2400	62,400	7,570
6	13200	2300	41800	4190	132,000	132,000
7	24600	----	78000	6720	246,000	21,200
Best Fit*	100	40	2200	100	25,000	1,000

\* As determined by comparing curves for various  $d$  values with the curves from reference 4 corresponding to the values of A and A/B indicated at the top of each column.

The values of  $d$  labeled "Best Fit" are determined by taking the curves in reference 4 for bending moment due to applied radial load  $C_{mr}$ , corresponding to the values of  $A$  and  $A/B$  indicated, and plotting them on top of page of curves of  $C_{mr}$  in reference 1.

The values of  $d$  indicated in Table C-1 are plotted vs.  $n$  in figure 8. The "Best Fit" values of  $d$  on each curve are joined by a dashed line, which is the desired curve giving  $n$  as a function of  $d$ . Values of  $n$  less than 2 were not permitted on theoretical grounds, and it was decided to keep  $n = 2$  for  $d \leq 110$ .

The relationship between  $\gamma$  and  $d$  is derived by substituting the relationship  $n = f(d)$  from figure 8 into equation (C.6).  $K_n$  is a known function of  $L_r/L_c$  and  $n$ . This enables curves of  $\gamma$  vs.  $d$  for various values of  $L_r/L_c$  to be plotted in figure 9.

Substantiation of this method of computing  $d$  was achieved by comparing a large number of curves in reference 4 with others computed from reference 1 using figure 9 and equation (C.1) to compute  $d$ . A few typical examples are shown in the figures.

The present method of computing  $d$  makes the curves in reference 1 practically identical to those in reference 4. Thus, the objection to the use of reference 4 for a heavily reinforced loaded frame supported by a shell with closely spaced frames carries over to the use of reference 1 for the same purpose. In view of the primitive idealization of shell action embodied in equation (C.2), it may be wondered whether the method of reference 1 has any value. Consider the problem of analyzing a very complex frame with non-uniform bending stiffness, cross-braces, etc. The solution of this problem is made tractable if it can be assumed that the supporting shell may be replaced by a set of simple springs whose stiffness is given by equation (C.2). Such a procedure is presented in reference 9. It has been shown in this Appendix that this procedure is rational provided that  $L$  is computed from figure 9 and equation (C.5).

#### Semi-Infinite Shell

From reference 1, but using the notation of this report,

$$\frac{\bar{v}_n(o)}{\bar{a}_n(o)} = \frac{\bar{u}_n(o)}{\bar{a}_n(o)} = \frac{L}{Gt} \quad (C.8)$$

Substituting equation (C.8) into equation (C.5), an expression is obtained for  $d$ :

$$d = \frac{r^4}{EI_o \bar{v}_n(o)/\bar{a}_n(o)} \quad (C.9)$$

The Input Impedance at the free end of a semi-infinite shell is given in equation (B.7), and on substituting it into equation (C.9):

$$\begin{aligned} d &= \frac{\sqrt{3} (n^3 - n)^2}{2\gamma n \sqrt{n^2 - 1} \sqrt{1 + \frac{(n^2 - 1)}{3} \left(\frac{L_r}{L_c}\right)^2}} \\ &= \frac{9}{\gamma \sqrt{1 + (L_r/L_c)^2}} \quad \text{for } n = 2 \end{aligned} \quad (C.10)$$

L-1028

It has been shown that for the infinite shell

$$d = \frac{36 \sqrt{1 + (L_r/L_c)^2}}{\gamma \left[ 1 + 2 (L_r/L_c)^2 \right]} \quad \text{for } n = 2$$

Thus, for small values of  $L_r/L_c$ ,  $d$ , for the semi-infinite shell, is approximately  $1/4$  that for the infinite shell, for that range in which  $n = 2$  dominates the solution. For values of  $d > 110$  it becomes necessary to account for the higher order stress systems, as has been done previously in this appendix, before comparing  $d$  for the infinite shell and semi-finite shell.

#### APPENDIX D

##### LOADS IN AN UNLOADED FRAME

Using the equilibrium equations of the shell [equations (1) to (4)], the frame bending moment per inch in the shell,  $m$ , and the other internal forces can be derived as functions of  $\ell/L_c$ . The bending moment at a frame, adjacent to a loaded frame, is obtained by multiplying  $m$  by  $I_\ell/i$ . The axial and shear forces in the frame can then be found by utilizing the equations of equilibrium of the frame.

From equations (1) to (4), the equilibrium equations of the shell, with "smeared out" frames, are:

$$\left. \begin{aligned} -\frac{\partial^2 s}{\partial \phi^2} &= \frac{\partial f}{\partial \phi} \\ \frac{\partial m}{\partial \phi} - s r &= 0 \\ \frac{1}{r} \frac{\partial^2 s}{\partial \phi^2} + \frac{\partial q}{\partial x} + \frac{s}{r} &= 0 \end{aligned} \right\} \quad (D.1)$$

Taking the case of a radially applied load and introducing the harmonic coefficients from equations (13) into (D.1), the equations for the harmonic coefficients are:

$$\left. \begin{aligned} -\frac{n^2 \bar{s}_n}{r} + \frac{\partial \bar{q}_n}{\partial x} + \frac{\bar{s}_n}{r} &= 0 \\ n \bar{m}_n + \bar{s}_n r &= 0 \end{aligned} \right\} \quad (D.2)$$

$$\bar{m}_n = -\frac{r^2}{n(n^2 - 1)} \frac{\partial \bar{q}_n}{\partial x} \quad (D.3)$$

A similar expression can be developed for  $\bar{m}_n$ , the analogous harmonic coefficient for the antisymmetric applied loading.  $\bar{q}_n$  is found from equations (43), and taking into account the antisymmetric case as well, the bending moment per inch becomes:

$$m = \sum_{n=2}^{n \leq N_c} \left[ \bar{q}_n(o) \cos n\phi + \bar{\bar{q}}_n(o) \sin n\phi \right] \frac{r^2 e^{-\alpha_n x}}{n(n^2 - 1)} \left\{ \alpha_n \left( \cos \beta_n x - \frac{(\alpha_n^2 - \beta_n^2)}{2\alpha_n \beta_n} \sin \beta_n x \right) + \beta_n \left( \sin \beta_n x + \frac{(\alpha_n^2 - \beta_n^2)}{2\alpha_n \beta_n} \cos \beta_n x \right) \right\} \\ + \sum_{n > N_c}^{\infty} \left[ \bar{q}_n(o) \cos n\phi + \bar{\bar{q}}_n(o) \sin n\phi \right] \frac{r^2}{n(n^2 - 1)} \left\{ \frac{\alpha_{1n}^3 e^{-\alpha_{1n} x} - \alpha_{2n}^3 e^{-\alpha_{2n} x}}{\alpha_{1n}^2 - \alpha_{2n}^2} \right\} \quad (D.4)$$

The bending moment in an unloaded frame at  $\ell$  is given by

$$M_\ell = \frac{I_\ell}{i} m(\ell) \quad (D.5)$$

The shear and axial forces in the unloaded frame are found from the equations of equilibrium for a frame, equations (50) to (52), with  $m_a = p_a = t_a = 0$ .

$$S = \frac{1}{r} \frac{dM}{d\phi} = \frac{1}{r} \cdot \frac{I_\ell}{i} \cdot \frac{dm}{d\phi} \quad (D.6)$$

$$F = -\frac{dS}{d\phi} = -\frac{1}{r} \cdot \frac{I_\ell}{i} \cdot \frac{d^2 m}{d\phi^2} \quad (D.7)$$

Substituting equation (D.4) into (D.5), (D.6), and (D.7) gives the bending moment, shear force and axial force in an unloaded frame, distance  $\ell$  from the loaded frame.

# APPENDIX E EFFECT OF ECCENTRICITY OF LOADED FRAME

## Introduction

The problem of a loaded frame whose neutral axis does not coincide with the skin line in a doubly infinite shell is considered in two parts. First, the "elementary beam theory" part is taken from reference 8 and modified slightly to agree with the sign conventions used in this report. Secondly, the solution for the "self-equilibrating" part is given in a form similar to the main text for the frame without eccentricity. This splitting up of the total solution is explained in the main text.

## Solution - "Elementary Beam Theory" Part

The table below is taken from reference 8.

	M	S	F
$P_o$	$\frac{P_o(1-\eta)r}{2\pi} \left[ 1 + \frac{\cos \phi}{2} - (\pi - \phi) \sin \phi \right]$	$\frac{P_o}{2\pi} \left[ (\pi - \phi) \cos \phi - \frac{2 \sin \phi}{(1-\eta)} + \frac{3}{2} \sin \phi \right]$	$\frac{P_o}{2\pi} \left[ \frac{2 \cos \phi}{(1-\eta)} - \frac{\cos \phi}{2} + (\pi - \phi) \sin \phi \right]$
$T_o$	$\frac{T_o(1-\eta)r}{2\pi} \left[ (\pi - \phi)(1 - \cos \phi) - \frac{3}{2} \sin \phi \right]$	$\frac{T_o}{2\pi} \left[ (\pi - \phi) \sin \phi + \frac{2 \cos \phi}{(1-\eta)} - \frac{5}{2} \cos \phi - (1 - \eta) \right]$	$\frac{T_o}{2\pi} \left[ \frac{2 \sin \phi}{(1-\eta)} - \frac{3}{2} \sin \phi - (\pi - \phi) \cos \phi \right]$
$M_o$	$\frac{M_o}{2\pi} \left[ (\pi - \phi) - 2 \sin \phi \right]$	$\frac{M_o}{2\pi(1-\eta)} \left[ (1 - \eta) + 2 \cos \phi \right]$	$-\frac{M_o \sin \phi}{\pi r(1 - \eta)}$

## General Solution - Self-Equilibrating Systems

Loaded Frame in a Doubly Infinite Shell

Assumptions. Except for there being an eccentricity  $g$  between the median plane of the skin and neutral axis of loaded frame, the assumptions are identical with those of the main text.

The equations of equilibrium are derived from figure 11. They are:

$$\frac{1}{r} \frac{dF}{d\phi} - \Delta q - \frac{1}{r} S + \frac{1}{r} t_a = 0 \quad (E.1)$$

$$\frac{dS}{d\phi} + F + p_a = 0 \quad (E.2)$$

$$\frac{dM}{d\phi} - S r - m_a + r^2 \eta \Delta q = 0 \quad (E.3)$$

Stress Strain Relations:

$$\frac{d\theta}{d\phi} = - \frac{M(1 - \eta)r}{EI_o} \quad (E.4)$$

Strain Displacement Relations:

Using the displacements  $v_{N.A.}$ ,  $w$  and  $\theta$  as the displacements of the neutral axis, as in the main text, we find that  $w$  and  $\theta$ , the radial and rotational deflections, respectively, are not affected by eccentricity. However,  $v$ , the tangential displacement at the skin line, is given by:

$$v = v_{N.A.} + \eta r \theta \quad (E.5)$$

Substituting this into the "inextensional" relations given as equations (54) and (55), we have

$$\frac{dw}{d\phi} = -v + \theta r \quad (E.6)$$

$$\frac{dv}{d\phi} - \eta r \frac{d\theta}{d\phi} = w \quad (E.7)$$

Combining these seven equations and introducing the harmonic coefficients, leads to a relationship between the tangential displacement and shear flow coefficients.

Firstly, eliminate  $w$  from equations (E.6) and (E.7)

$$\frac{1}{r} \left\{ \frac{d^3 v}{d\phi^3} + \frac{dv}{d\phi} \right\} = \eta \frac{d^3 \theta}{d\phi^3} + \frac{d\theta}{d\phi} \quad (\text{E. 8})$$

Using equations (E.4) and (E.8), we have

$$\frac{1}{r} \left\{ \frac{d^3 v}{d\phi^3} + \frac{dv}{d\phi} \right\} = - \frac{(1-\eta)r}{EI_o} \left\{ \eta \frac{d^2 M}{d\phi^2} + M \right\} \quad (\text{E. 9})$$

Combining equation (E.1) and (E.2)

$$\Delta q = - \frac{1}{r} \left\{ \frac{d^2 S}{d\phi^2} + S \right\} + \frac{1}{r} \left\{ t_a - \frac{dp_a}{d\phi} \right\} \quad (\text{E. 10})$$

From equation (E.3) obtain expressions for  $d^2 S/d\phi^2$  and  $S$ , which are substituted into equation (E.10) to give

$$\left\{ 1 + \frac{\eta}{1-\eta} \left( \frac{d^2 \Delta q}{d\phi^2} + \Delta q \right) \right\} = \frac{1}{r} \left\{ t_a - \frac{dp_a}{d\phi} \right\} - \frac{1}{(1-\eta)r^2} \left\{ \frac{d^3 M}{d\phi^3} + \frac{dM}{d\phi} - \frac{d^2 m_a}{d\phi^2} - m_a \right\} \quad (\text{E. 11})$$

At this juncture, consider the effects of symmetry and introduce the harmonic coefficients.

#### Applied Radial Load

Introducing the harmonic coefficients (see the main text) into equations (E.9) and (E.11) and noting that  $m_a = t_a = 0$  leads to:

$$\bar{M}_n = \frac{(n^3 - n)EI_o \bar{v}_n}{r^2(1-\eta)(1-\eta n^2)} \quad (\text{E. 12})$$

and

$$\bar{\Delta q}_n \left\{ 1 - \frac{\eta(n^2 - 1)}{(1-\eta)} \right\} = - \frac{(n^3 - n)\bar{M}_n}{(1-\eta)r^2} + \frac{nP_o}{\pi r} \quad (\text{E. 13})$$

Substituting equation (E.12) into equation (E.13) and noting that  $\bar{q}_n(0) = \bar{\Delta q}_n/2$ , in the case of a doubly infinite shell, we have

$$\bar{q}_n(0) \left\{ 1 - \frac{\eta(n^2 - 1)}{(1-\eta)} \right\} = - \frac{(n^3 - n)^2 EI_o \bar{v}_n}{2(1-\eta)^2 r^4 (1-\eta n^2)} + \frac{nP_o}{2\pi r} \quad (\text{E. 14})$$

For the shell, we have from equation (49),

$$\bar{u}_n(o) = \frac{r^4 K_n}{Ei(n^3 - n)^2 L_c} \bar{q}_n(o) \quad (E. 15)$$

Combining equation (E. 15) and equation (E. 14) gives

$$\bar{q}_n(o) = \frac{\frac{nP_o}{2\pi r}}{\left\{ 1 - \frac{\eta(n^2 - 1)}{(1 - \eta)} + \frac{\gamma K_n}{(1 - \eta)^2 (1 - \eta n^2)} \right\}} \quad (E. 16)$$

Equation (E. 16) can be rewritten as

$$\bar{q}_n(o) = \frac{\frac{nP_o}{2\pi r} \left( \frac{1 - \eta}{1 - \eta n^2} \right)}{(1 + \gamma^* K_n)}$$

where

$$\gamma^* = \frac{\gamma}{(1 - \eta)(1 - \eta n^2)^2}$$

#### Applied Moment and Tangential Load

Taking due account of antisymmetry and carrying out similar operations as for the radial load

$$\bar{\bar{q}}_n(o) = \frac{-\frac{1}{2\pi} \left\{ \frac{T_o}{r} - \frac{(n^2 - 1)}{r^2} M_o \right\} \left( \frac{1 - \eta}{1 - \eta n^2} \right)}{(1 + \gamma^* K_n)}$$

By using these modified shear-flow harmonic coefficients in the manner given in the main text, the entire solution to the problem can be generated.



## REFERENCES

1. Wignot, J. E., Combs, H., and Ensrud, A. F.: Analysis of Circular Shell-Supported Frames, NACA TN 929, July 1943.
2. Hoff, N. J.: "Stresses In A Reinforced Monocoque Cylinder Under Concentrated Symmetric Transverse Load," Jour. of Applied Mechanics, vol. II, no. 4, December 1944, p. A-235.
3. Duberg, J. E., and Kempner, J.: Stress Analysis by Recurrence Formula of Reinforced Circular Cylinders Under Lateral Loads, NACA TN 1219, 1947.
4. Kempner, J., and Duberg, J. E.: Charts for the Stress Analysis of Reinforced Circular Cylinders Under Lateral Loads, NACA TN 1310, May 1947.
5. Dwight, H. B.: Tables of Integrals and Other Mathematical Data, The Macmillan Company, 1955.
6. MacNeal, Richard H., and Bailie, John A.: Analysis of Frame-Reinforced Cylindrical Shells. Part II - Discontinuities of Circumferential-Bending Stiffness in the Axial Direction. NASA TN D-401, 1960.
7. MacNeal, Richard H., and Bailie, John A.: Analysis of Frame-Reinforced Cylindrical Shells. Part III - Applications. NASA TN D-402, 1960.
8. Fahlbusch, H., and Wegner, W.: Stress Analysis of Circular Frames, NACA TM 999, 1941.
9. Dallison, K. J.: Stress Analysis of Circular Frames in a Non-tapering Fuselage. J.R.Ae.S. March 1953.

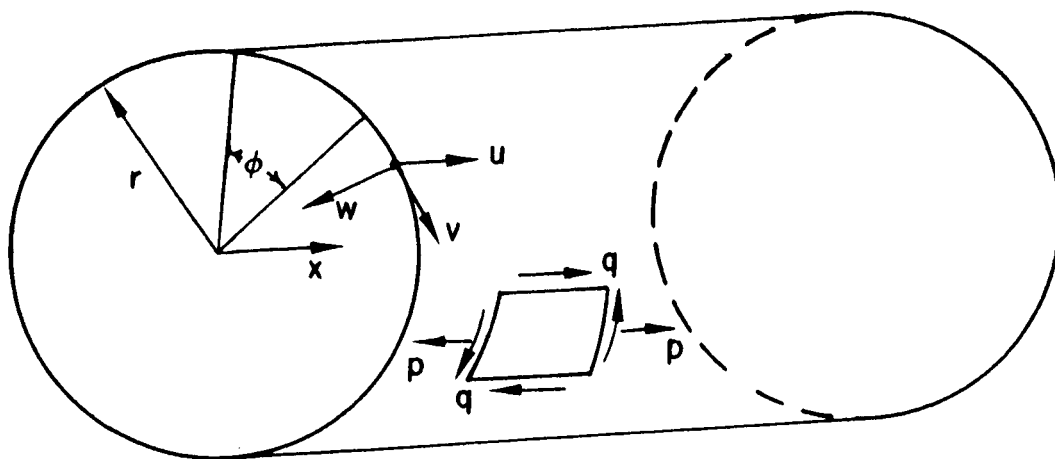


Figure 1. - Loads per inch and displacements in the shell.

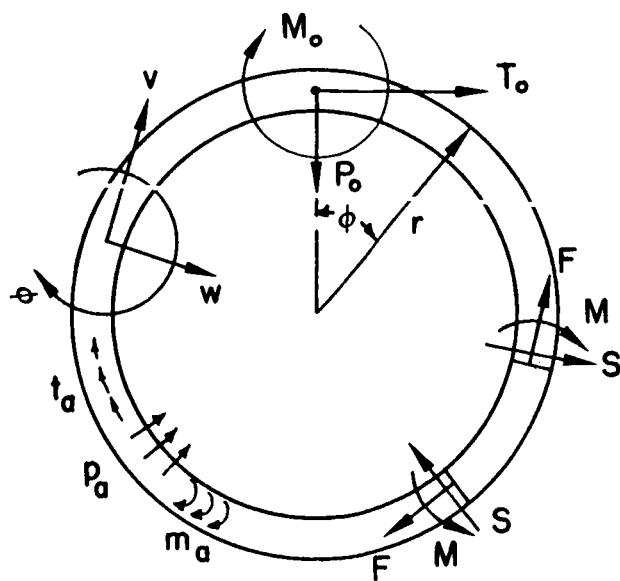


Figure 2. - Externally loaded frame.

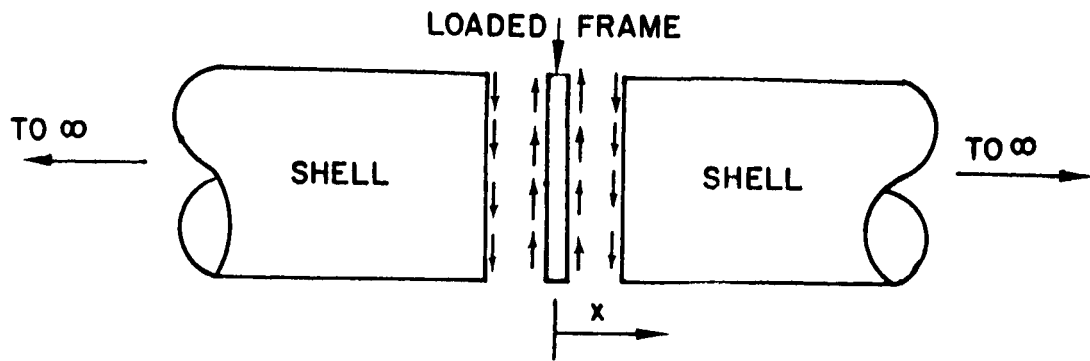


Figure 3. - An exploded view of the shell.

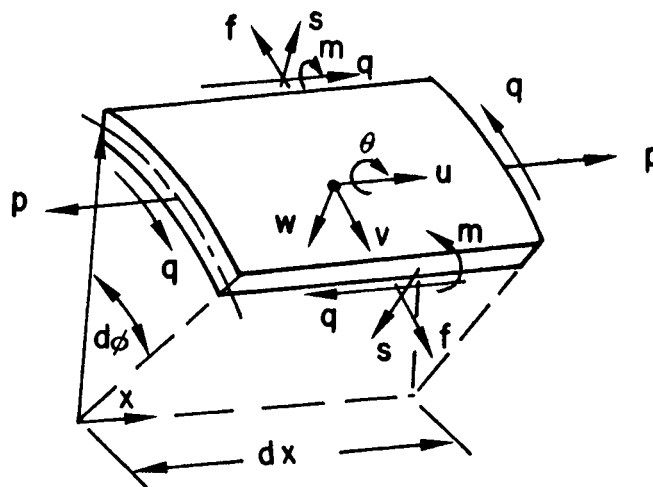


Figure 4. - Loads per inch and displacements in the shell.

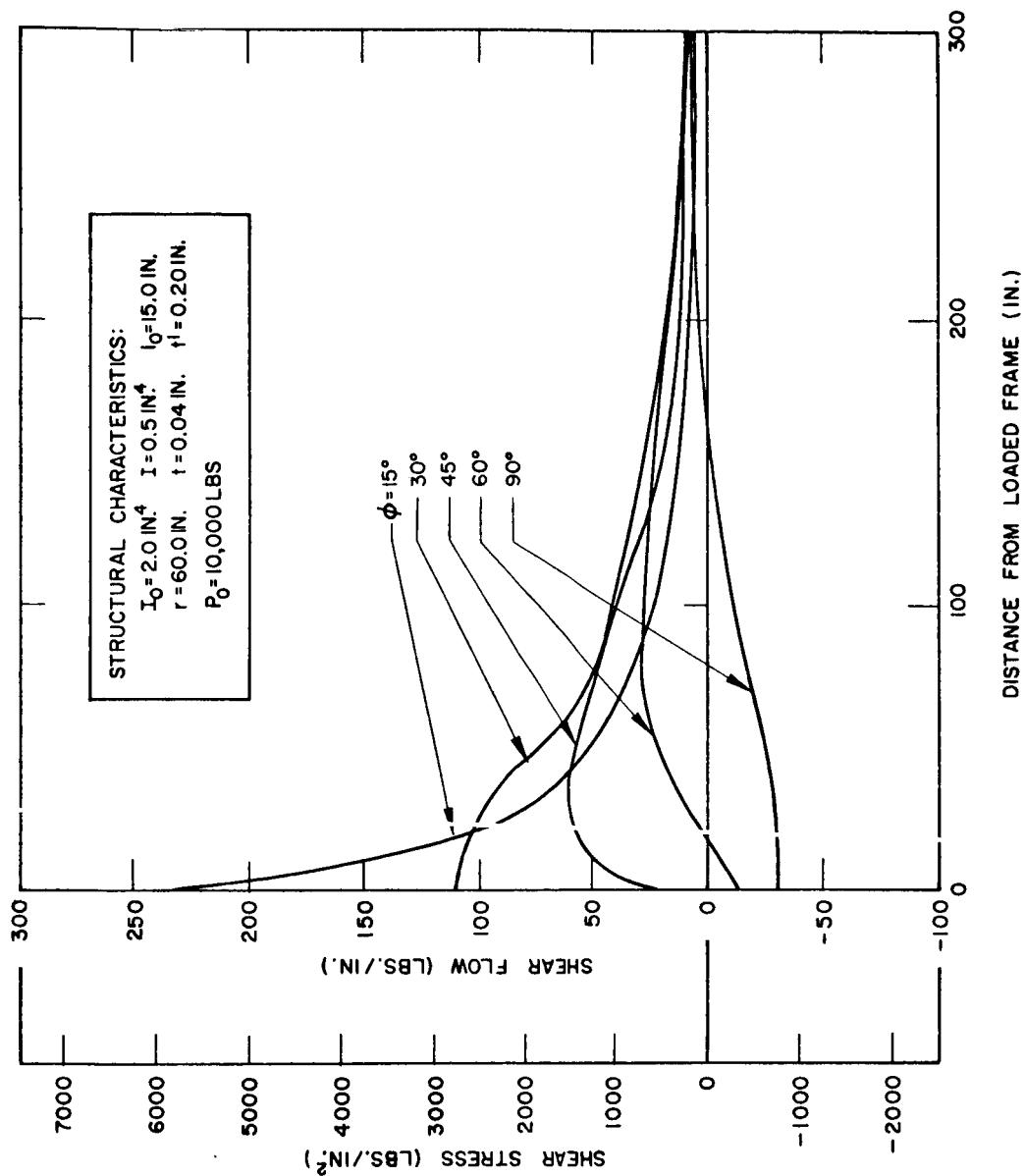


Figure 5. - An example to illustrate the magnitude of shear flow and shear stress in a shell due to frame flexibility only.

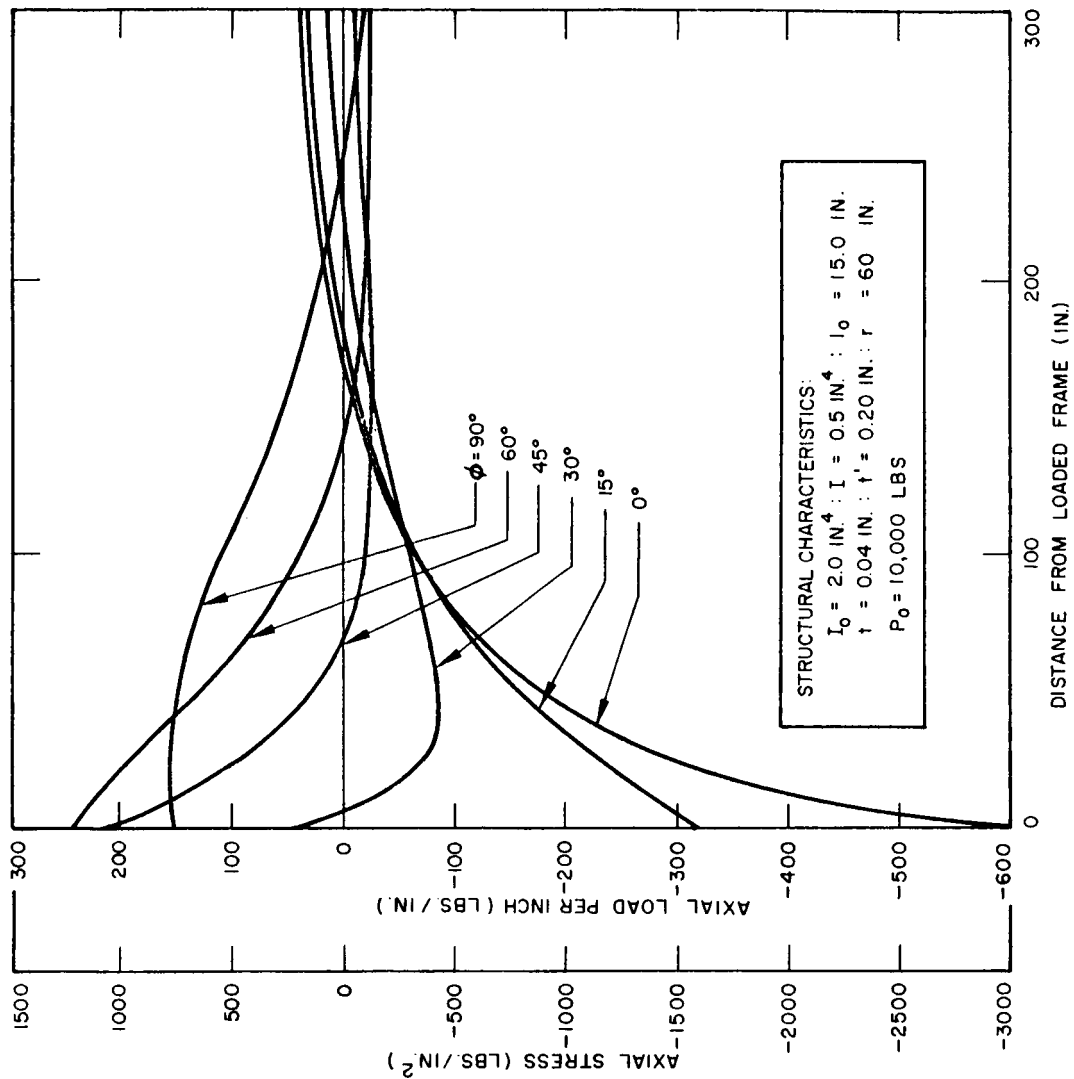


Figure 6. - An example to illustrate the magnitude of axial load per inch and axial stress in a shell due to frame flexibility only.

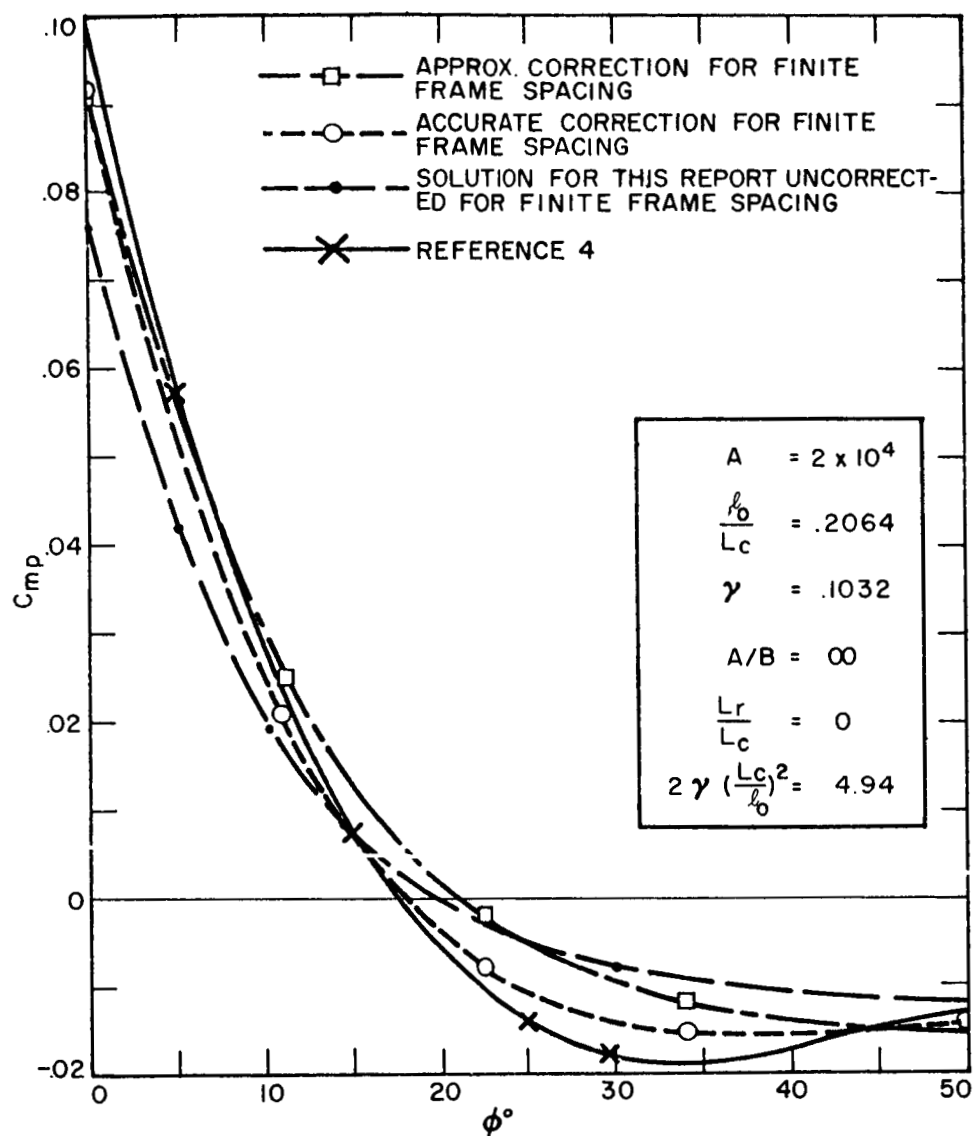


Figure 7. - An example to illustrate magnitude of correction due to finite frame spacing.

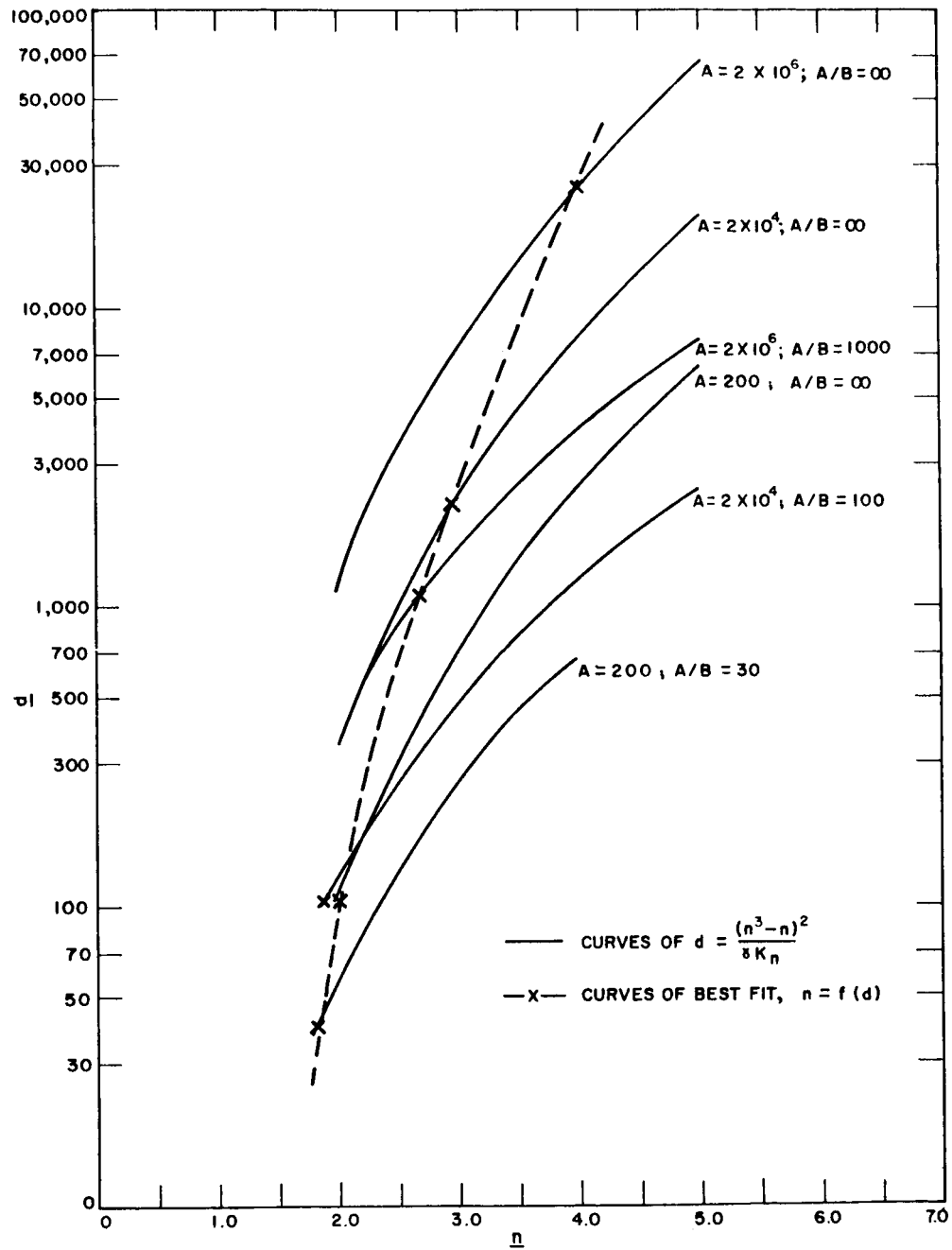


Figure 8. - Relationship between parameters of this report and those of reference 1.

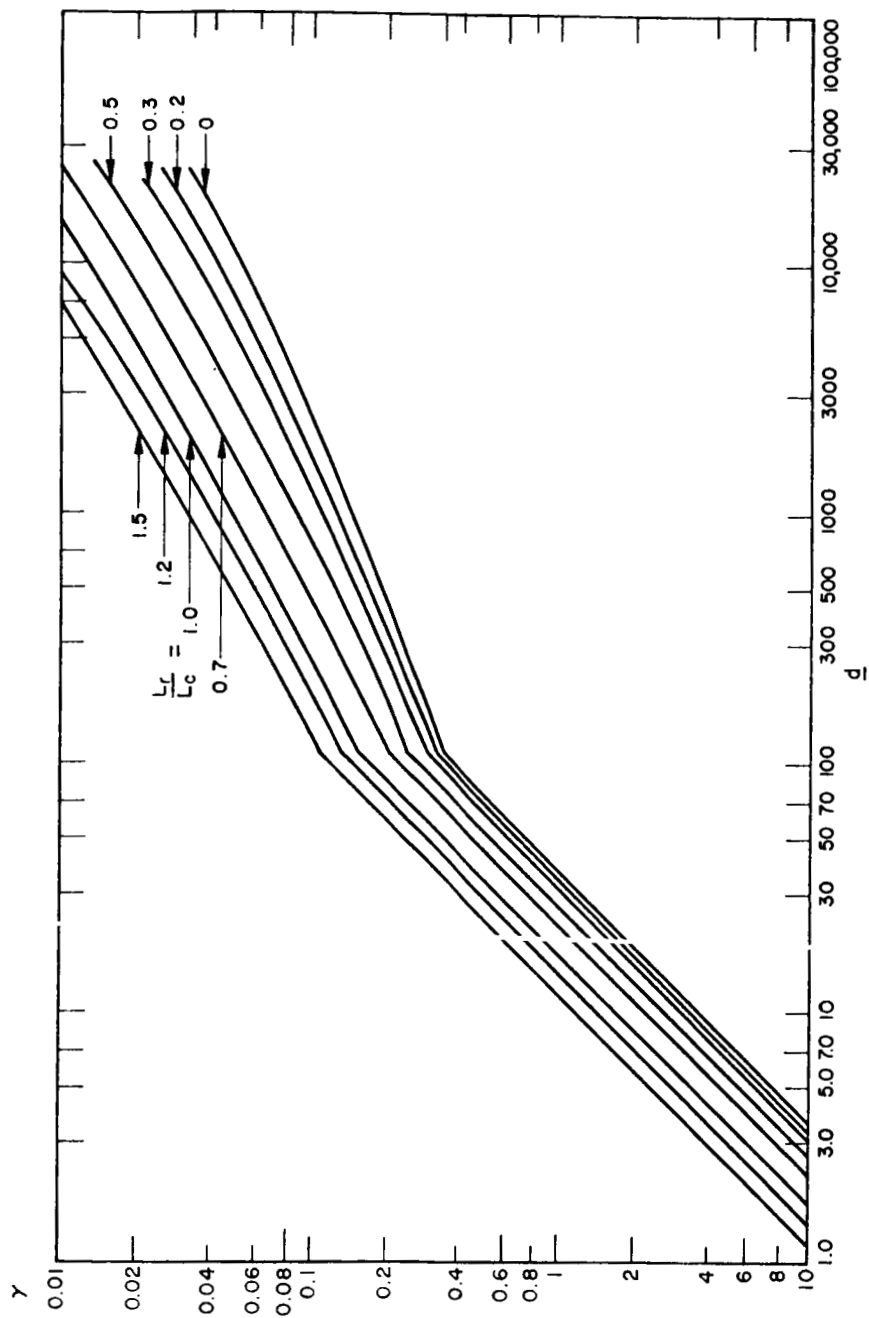


Figure 9. - Chart for determining parameter "d" of reference 1.



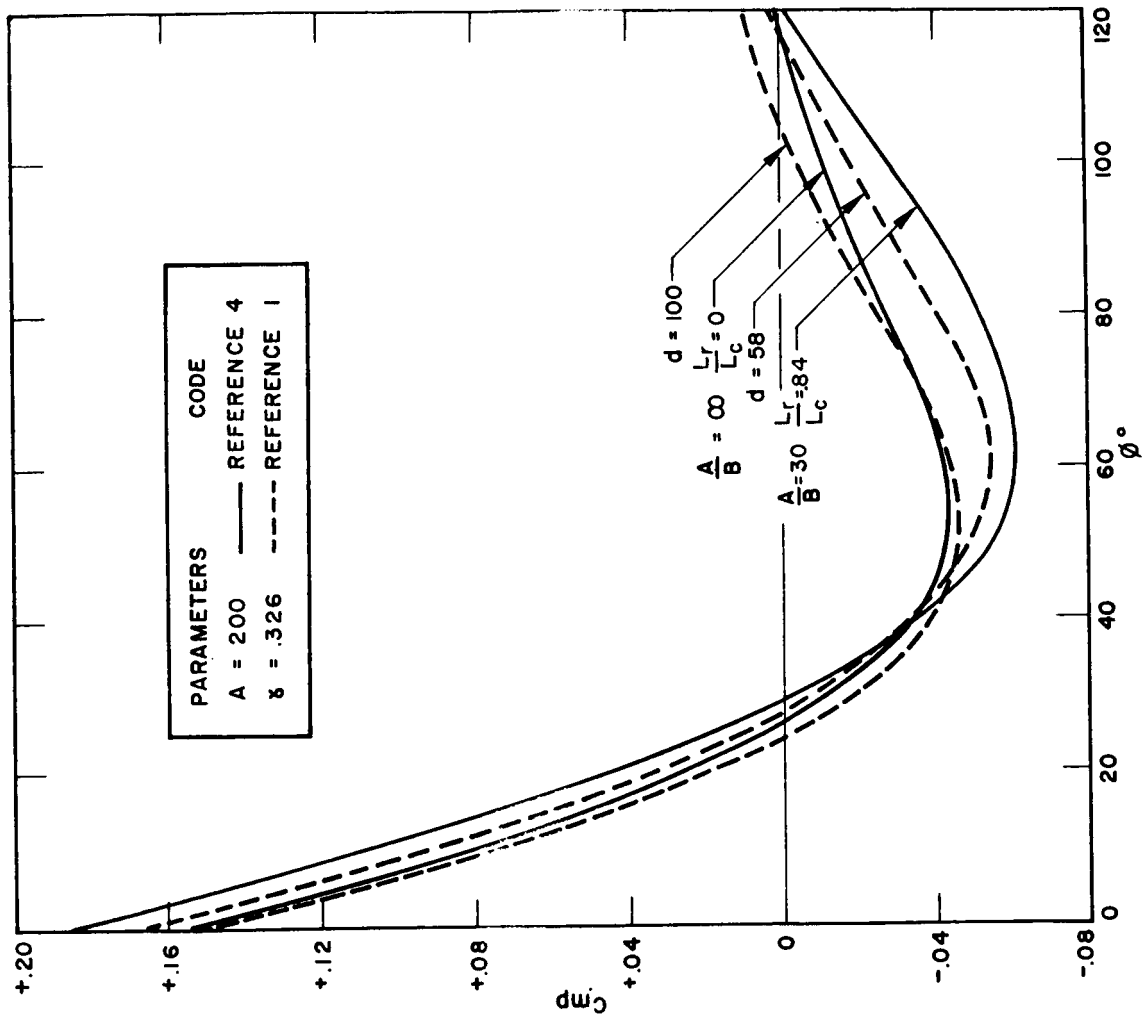


Figure 10. - A typical comparison of references 4 and 1 using "d" derived by method of this report.

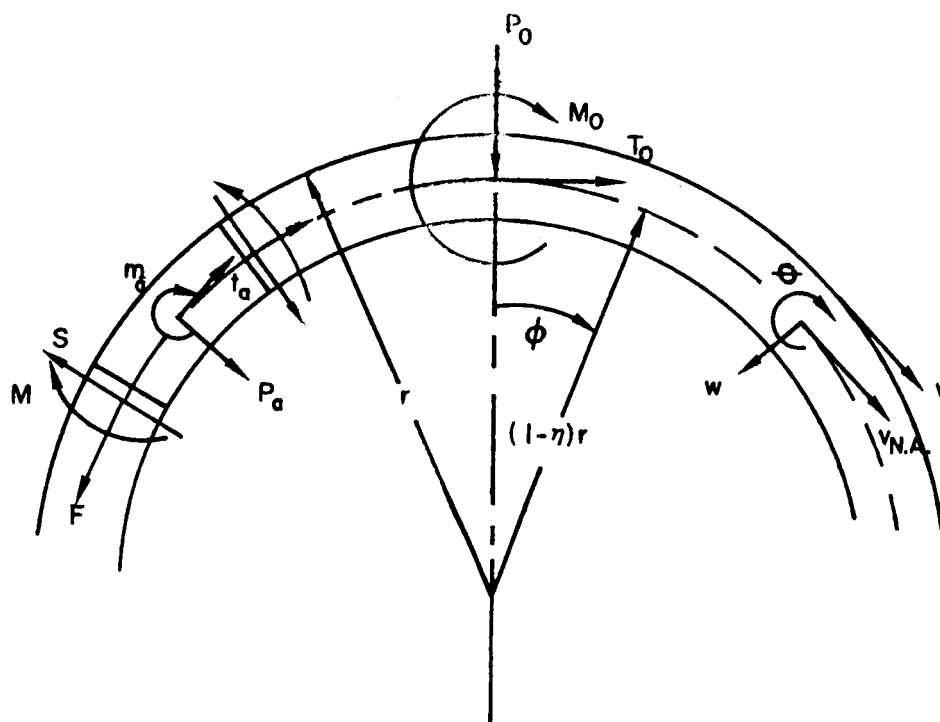


Figure 11. - Loads and displacements in the frame accounting for eccentricity between skin and frame neutral axis.